Long-term evolution of an accretionary prism: The case study of the Shimanto Belt, Kyushu, Japan

Hugues Raimbourg, Romain Augier, Vincent Famin, Leslie Gadenne, Giulia Palazzin, Asuka Yamaguchi, Gaku Kimura

AGU PUBLICATIONS

Tectonics

RESEARCH ARTICLE
10.1002/2013TC003412

Key Points:
- Five stages of deformation were recognized in the Shimanto Belt
- Two stages of extension alternated with compression
- The Shimanto Belt is not a simple, giant accretionary prism

Correspondence to:
H. Raimbourg,
hugues.raimbourg@univ-orleans.fr

Citation:
Raimbourg, H., R. Augier, V. Famin, L. Gadenne, G. Palazzin, A. Yamaguchi, and G. Kimura (2014), Long-term evolution of an accretionary prism: The case study of the Shimanto Belt, Kyushu, Japan, *Tectonics*, *33*, doi:10.1002/2013TC003412.

Received 18 JUL 2013
Accepted 25 APR 2014
Accepted article online 6 MAY 2014

Long-term evolution of an accretionary prism: The case study of the Shimanto Belt, Kyushu, Japan

Hugues Raimbourg[1,2], Romain Augier[1], Vincent Famin[3], Leslie Gadenne[1], Giulia Palazzin[1], Asuka Yamaguchi[4], and Gaku Kimura[5]

[1]ISTO, Institut des Sciences de la Terre d'Orléans, UMR 7327, CNRS/Université d'Orléans/BRGM, Orléans, France, [2]IFREE, Japan Agency for Marine-Earth Science and Technology, Yokosuka, Kanagawa, Japan, [3]Laboratoire Géosciences Réunion—IPGP, Université de la Réunion, La Réunion, France, [4]Atmosphere and Ocean Research Institute, University of Tokyo, Kashiwa, Chiba, Japan, [5]Department of Earth and Planetary Science, University of Tokyo, Bunkyo-ku, Tokyo, Japan

Abstract The Shimanto Belt in SW Japan is commonly described as a paleo-accretionary prism, whose structure is explained by continuous accretion like in modern accretionary prisms such as Nankai. We carried out a structural study of the Cretaceous to Miocene part of the Shimanto Belt on Kyushu to test this hypothesis of continuous accretion. Most deformation structures observed on the field are top-to-the-SE thrusts, fitting well the scheme of accretionary wedge growth by frontal accretion or underplating. In particular, the tectonic mélange at the top of the Hyuga Group records a penetrative deformation reflecting burial within the subduction channel. In contrast, we documented two stages of extension that require modifying the traditional model of the Belt as a "simple" giant accretionary wedge. The first one, in the early Middle Eocene, is mostly ductile and localized in the foliated bases of the Morotsuka and Kitagawa Groups. The second one, postdating the Middle Miocene, is a brittle deformation spread over the whole belt on Kyushu. Integrating these new tectonic features to existing data, we propose 2-D reconstructions of the belt evolution, leading to the following conclusions: (1) Erosion and extension of the margin in the early Middle Eocene resulted from the subduction of a trench-parallel ridge. (2) The Late Eocene to Early Miocene evolution is characterized by rapid growth of the prism, followed by a Middle Miocene stage where large displacements occurred along low-angle out-of-sequence thrusts such as the Nobeoka Tectonic Line. (3) From middle Miocene, the strain regime was extensional.

1. Introduction

Subduction zones can be either accretive or erosive [*Von Huene and Scholl*, 1991], depending on whether material is added to or removed from the subducting plate. Arguments in favor of subduction erosion include subsidence of the margin or landward displacement of arc volcanism, as was described for example in northern Japan [*Von Huene and Lallemand*, 1990]. In contrast, the southwestern margin of Japan, above the subducting Philippine sea plate, is considered as a typical example of an accretive margin, directly imaged and studied through several seismic and ocean drilling campaigns. Seismic transects off Muroto cape revealed the presence of a thick accretionary prism (Nankai accretionary prism) fed by the frontal accretion of incoming sedimentary material above a décollement zone extending seaward of the deformation front [*Moore et al.*, 2001, 2005]. The structure of the frontal part of the prism is somehow different along the recently studied Kumano transect off Kii Peninsula, as the whole incoming sedimentary sequence is currently being subducted [*Moore et al.*, 2009], but the overlying prism still incorporates young trench wedge sediments recently accreted [*Expedition 316 Scientists*, 2009].

The biostratigraphy of cores drilled in the Nankai accretionary prism enabled the accreted material to be dated back to the late Miocene [*Expedition 319 Scientists*, 2010]. Even taking into account deeper drillings possible in the near future, investigation focused on the offshore portion of the margin shall provide no information on its evolution beyond ~10 Ma. The long-term evolution of the margin relies necessarily on onland exposures, often considered as fossil structures.

The Shimanto Belt is the onland prolongation of the modern Nankai accretionary prism [*Taira*, 1981; *Tanaka and Nozawa*, 1977] and provides therefore the opportunity to analyze the long-term evolution of a margin in convergent settings. The nature of the material involved in the belt (i.e., sediments with facies correlable to

active margins or abyssal plains and a limited amount of oceanic crust), the distribution of ages that shows a general younging trend of biostratigraphic ages toward the current trough, and the repetition of units revealing numerous thrusts led several authors to define the Shimanto Belt as a "mega" accretionary prism built by accretion from Late Cretaceous to Early Miocene times [*Isozaki et al.*, 2010; *Sakai and Kanmera*, 1981; *Sakai et al.*, 1984; *Sakai*, 1985; *Taira et al.*, 1980a, 1980b, 1988]. Accretion may have been discontinuous with several pulses rather than with a steady fashion [*Isozaki et al.*, 2010].

This interpretation has been criticized by *Charvet and Fabbri* [1987] and *Charvet* [2013], for whom the geodynamic evolution of Japanese islands from the Late Paleozoic to the Early Cenozoic complies with a succession of collisions of continental microblocks, separated by periods of oceanic subduction. In addition to arguments about the typical continental isotopic signature of Middle Miocene magmatism [*Jahn*, 2010] and the mechanical viability for ridge or seamount subduction to trigger accretion, *Charvet* [2013] proposes a number of tectonic arguments against the accretion model applied to Shimanto. In particular, the large-scale contacts and their relative chronology are more akin to nappe transports typical of collisional orogens rather than to accretionary prisms.

In order to understand the long-term evolution of the Shimanto Belt, notwithstanding the insights of indirect methods such as dating of detrital zircons [*Isozaki et al.*, 2010; *Nakama et al.*, 2010], the study of deformation at all scales is essential. Such an analysis, which has been done in detail for example for the Sambagawa Belt [*Faure,* 1985a, 1985b; *Wallis*, 1998], is limited for the Shimanto Belt on Kyushu to the base of the Cretaceous unit (i.e., Morotsuka Group; [*Fabbri et al.*, 1987; *Toriumi and Teruya*, 1988]). The lateral portion of the Shimanto Belt on Shikoku has been more studied, but even there, the structural work is restricted to a few regional cross sections along the coast with a limited length, at most a few kilometers [*DiTullio and Byrne*, 1990; *Hashimoto and Kimura*, 1999; *Ikesawa et al.*, 2005; *Kitamura et al.*, 2005]. To date, there is thus no integrated study encompassing the whole belt and interpreting its long-term geodynamic evolution.

To reach this goal, we have carried out on Kyushu a large-scale structural study of the deformation recorded in the Late Cretaceous and early to mid-Cenozoic Shimanto Belt. The main structures were followed along several seriated cross sections, which unraveled the dominant features of the deformation and along-strike variations.

The result of this structural analysis, described in the first part of the paper, yielded five deformation stages, three of them compatible with the "predicted" dynamics of a prism growing oceanward by frontal accretion and underplating and two other ones pointing out to a completely different geodynamic framework. We have then combined these data with the existing ones, in particular concerning the Takachiho tectonic stage in Early Miocene or the extension affecting the Miyazaki Group that unconformably overlays the Shimanto Belt, to interpret these deformation stages into the belt evolution and to build 2-D reconstructions of the evolution of the Shimanto Belt from Late Cretaceous times.

2. Geological Settings

2.1. Anatomy of the Shimanto Belt

The northern part of the Shimanto Belt on Kyushu is divided into three subbelts or groups with respect to their stratigraphic ages and relative tectonic position: the Morotsuka, Kitagawa, and Hyuga Groups (Figure 1). Available geological data are all compiled in Table 1. Farther south, the Shimanto Belt includes the Nichinan Group, composed of intercalated coherent turbidite units and mélange units [*Sakai*, 1985]. On top of the Shimanto lies unconformably the Miyazaki Group, a thick coherent turbiditic sequence [*Murata*, 1997].

The Morotsuka Group, of Cretaceous age, is divided into two subgroups, from north to south [*Teraoka and Okumura*, 1992]: the sandstone-rich Saiki Subgroup, of Hauterivian/Barremian to Coniacian/Santonian age, and the mudstone-rich Kamae Subgroup, whose age ranges from Cenomanian to Campanian/Maastrichtian (Table 1). In the Shiibamura district, the Kamae Subgroup ages range in Cenomanian-Turonian, the same as the overlying, sandstone-rich, lower unit of the Saiki Subgroup [*Saito et al.*, 1996]. It is noteworthy that the names and divisions within the Morotsuka Group differ depending on the authors: Saiki (Kamae) becomes Morotsuka (Makimine) in *Murata* [1997], while the Kamae Subgroup is described as the foliated base of the whole Cretaceous Shimanto in *Charvet and Fabbri* [1987] and *Fabbri et al.* [1987]. The Morotsuka and

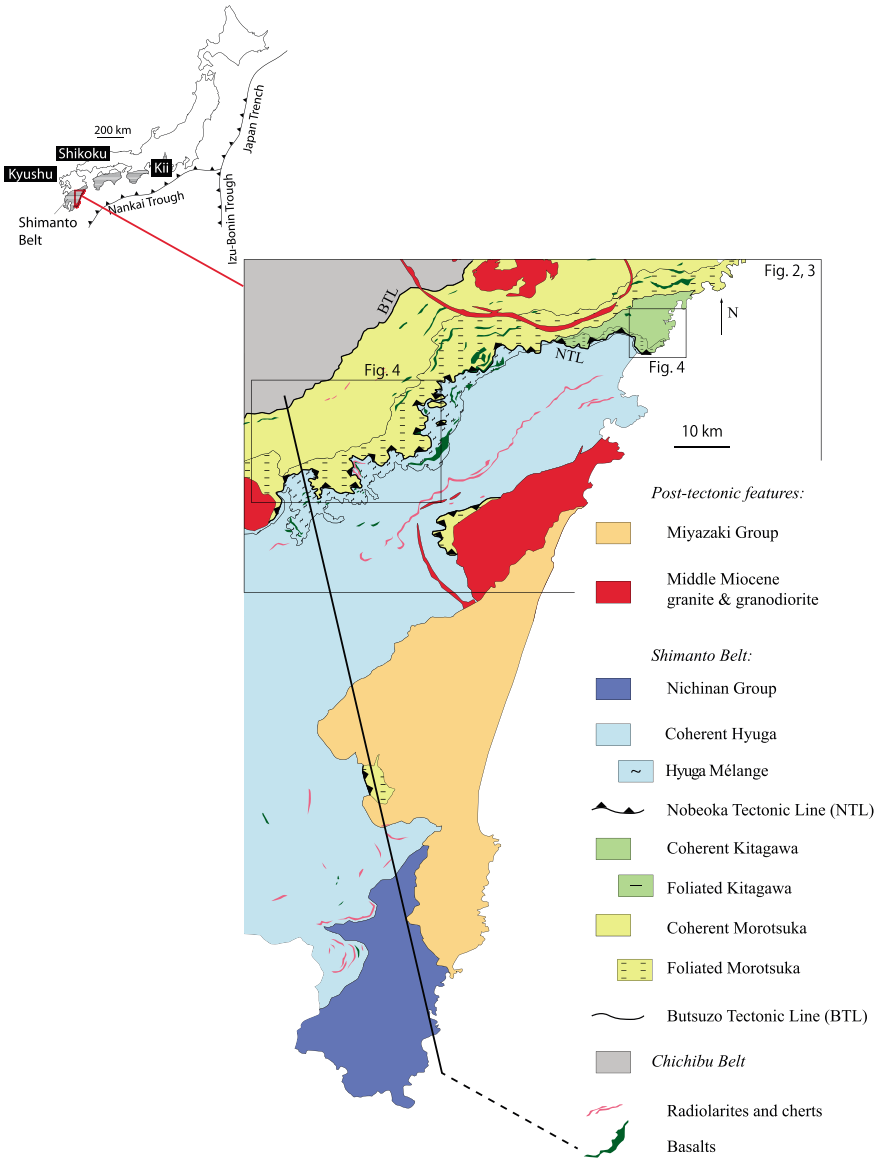

Figure 1. Map of the Shimanto Belt on Kyushu (adapted from *Murata* [1997], limited by the border of the Miyazaki prefecture and the coast line). The Nobeoka Tectonic Line (NTL) separates Cretaceous (Morotsuka Group) or Eocene (Kitagawa Group) units of higher grade in the hanging wall from lower grade, post Middle Eocene units (Hyuga and Nichinan Groups) in the footwall. The cross section of the whole belt in Figure 11 corresponds to the NW-SE trending line.

Kitagawa Groups share a roughly similar internal structure, divided into three lithostratigraphic formations (from bottom to top): a basal formation constituted of blocks of sandstone and pillow basalts embedded in a clay-rich matrix; an intermediate formation made of fine-grained, thin, and well-bedded turbidites; and an upper formation dominantly made of coarser grained turbidites with massive sandstone layers [*Sakai and Kanmera*, 1981].

Deposition ages for the Kitagawa Group are constrained by the presence of Eocene radiolarians in the lower formation of the Kitagawa Group [*Ogawauchi et al.*, 1984].

The Hyuga Group extends from the end of the Middle Eocene (Foraminifera zone P14) to the end of the Early Oligocene (zone P20) [*Sakai et al.*, 1984]. Its structurally upper formation is a mélange of various blocks and slivers (sandstones, pillow basalts, red shales, and cherts), dated from the Middle Eocene [*Sakai et al.*, 1984], embedded in a heavily sheared dark pelitic matrix of Late Eocene to Early Oligocene, called either the Aradani formation [*Sakai et al.*, 1984] or the Mikado formation [*Teraoka et al.*, 1981]. It overlies

AGU Tectonics

10.1002/2013TC003412

Table 1. Summary of Available Constraints on the Different Units (From North to South), Including Biostratigraphic and Radiometric Ages and Rock Maximum Temperature[a]

Unit	Biostratigraphic Age	Reference	Comments	Radiometric Age (Ma)	Method	Reference	T_{max} (°C)	Method	Reference
Coherent Morotsuka	Hauterivian/Barremian to Coniacian/Santonian	[a]	named "Saiki Subbelt"	13.3 ± 3.9 (±2σ)	Fission tracks in apatite	[g]	280–300	Illite cristallinity	[h]
Foliated Morotsuka	Cenomanian to Campanian/Maastrichtian	[a]	named "Kamae Subbelt"	7.1 ± 2.3, 8.8 ± 6.5 (±2σ)	Fission tracks in apatite	[g]	300 ± 30	Illite cristallinity	[j]
	Cenomanian to Turonian	[b]	In Shiibamura district	58.1 ± 2.9, 54.9 ± 2.7, 48.7 ± 2.4, 49.0 ± 2.4	K-Ar on illite	[h]	300–310	Illite cristallinity	[h]
				46.4 ± 2.6, 47.9 ± 2.5 (±1σ)	Fission tracks in zircon	[h]	□		
Foliated Kitagawa	Eocene	[c]		48.4 ± 1	K-Ar on mica in metamorphic cleavage	[i]	300 ± 30	Illite cristallinity	[j]
							320–330	Vitrinite reflectance	[k]
Hyuga Mélange	Late Eocene to Early Oligocene	[d]	Foraminifera zones P15 to P18–Blocks of early middle Miocene	7.6 ± 4.1 (±2σ)	Fission tracks in apatite	[g]	250–270 ± 30	Illite cristallinity	[j]
	Middle to Late Eocene	[e]	Foraminifera zones P13 to P17				260–300	Illite cristallinity	[h]
							250–270	Vitrinite reflectance	[k]
Coherent Hyuga	Late Eocene to late Early Oligocene	[d]	Foraminifera zones P15 to P20				230–290	Illite cristallinity	[h]
	late Middle Eocene to late Early Oligocene	[e]	Foraminifera zones P13 to P21a						
Nichinan	Late Oligocene to Early Miocene	[f]							
	late Early Oligocene to Early Miocene	[d]	Foraminifera zones P20 to N4						
Miyazaki Group	Late Miocene to Pliocene	[f]							

[a]References are [a]: [*Teraoka and Okumura*, 1992], [b]: [*Saito et al.*, 1996], [c]: [*Ogawauchi et al.*, 1984], [d]: [*Sakai et al.*, 1984], [e]: [*Nishi*, 1988], [f]: [*Sakai*, 1985], [g]: [*Hasebe and Tagami*, 2001], [h]: [*Hara and Kimura*, 2008], [i]: [*Mackenzie et al.*, 1990], [j]: [*Mukoyoshi et al.*, 2009], and [k]: [*Kondo et al.*, 2005].

various coherent units, composed of a varying proportion of mudstones and sandstones, from black shales to turbidites with massive sandstone beds [*Murata*, 1997; *Sakai and Kanmera*, 1981].

The Nichinan Group extends from the Late Oligocene (zone P20) to the Early Miocene (nannofossil zone N4) [*Sakai et al.*, 1984] and the Miyazaki Group from the Late Miocene to the Pliocene (zone N15 to zone N20/21 [*Sakai*, 1985]).

For the sake of clarity, we refer hereafter to the different units by their dominant nature and morphology, instead of using formation names, which differ depending on the authors and the geographic position. The Morotsuka and Kitagawa Groups are thus divided (from top to bottom) into an upper, turbidite-rich formation where the sedimentary bedding is the dominant fabric ("Coherent Morotsuka" and "Coherent Kitagawa") and a lower, clay-rich foliated formation ("Foliated Morotsuka" and "Foliated Kitagawa"), while the Hyuga Group is divided into a mélange formation ("Hyuga Mélange," below the Nobeoka Tectonic Line (NTL)), which overlies a thick succession of alternating sandstone-rich and mudstone-rich formations, where the sedimentary bedding is the dominant fabric ("Coherent Hyuga").

2.2. Overall Geometry and First-Order Structures

All the formations within the groups described above present a general northwestward dipping structure and an overall northwestward younging (i.e., normal stratigraphic polarity). In contrast, within each group, the younger formations are stacked underneath the older ones, resulting in a general younging direction downsection, i.e., toward the southeast, as for example within the Hyuga Group [*Nishi*, 1988; *Sakai et al.*, 1984]. At the scale of the whole belt, considering the set of Morotsuka, Kitagawa, Hyuga, and Nichinan Groups, younging direction is also downsection, toward the southeast.

The contacts between these groups are presumably tectonic, and the NTL is the largest scale and the clearest example of such contacts in the Shimanto Belt. The NTL crops out over more than 100 km on Kyushu and extends eastward on Shikoku. It separates the Morotsuka and Kitagawa Groups in the north (i.e., hanging wall unit) from the Hyuga Group in the south (i.e., footwall unit). In large-scale cross sections, the NTL is a low dipping thrust [*Murata*, 1997; *Saito et al.*, 1996], in agreement with outcrop-scale observations where the NTL is a low-dip angle, ~10 cm thick cataclastic zone that cuts across the main fabric of both the hanging wall and the footwall units [*Mukoyoshi et al.*, 2009]. As reported by these authors, kinematics observed on the field reveal a consistent top-to-the-SE motion of the Morotsuka/Kitagawa Group with respect to the Hyuga Group. The two main klippes [*Murata*, 1997] underlain by the NTL argue in favor of a large amount of movement, further supported by the gap across it, either in terms of metamorphic grade (actinolite facies above versus prehnite-pumpellyite facies below [*Imai et al.*, 1971; *Toriumi and Teruya*, 1988]) or deposition age (Cretaceous above versus Eocene below [*Sakai and Kanmera*, 1981; *Sakai et al.*, 1984]).

In contrast to the NTL, the other large-scale thrusts mapped on the geological maps or on previous studies were not observed.

At smaller scale (approximately hundreds of meters), imbricate thrusting involving the multiple repetition of the same thrust sheet was unraveled by biostratigraphic analysis, such as was done along the Mimi River [*Nishi*, 1988; *Sakai et al.*, 1984] or by the correlation of lithostratigraphic columns [*Sakai and Kanmera*, 1981].

2.3. Deformation Stages

The main tectonic phase, observed throughout the Shimanto Belt, is characterized by south verging asymmetrical folds and thrusts [*Charvet and Fabbri*, 1987; *Murata,* 1996, 1998]. This phase is referred to by these authors as the "Takachiho phase," in the Early to Middle Miocene [*Sakamoto*, 1977; *Tanaka and Nozawa*, 1977]. In Kyushu, the age of the major compression stage of the Takachiho phase is crudely bracketed by the youngest stratigraphic ages of the folded Nichinan Group (zone N5, ~25–20 Ma) and by the intrusion of the undeformed Osuzuyama magmatic complex dated at approximately 14 Ma [*Shibata and Nozawa*, 1982; *Tanaka and Nozawa*, 1977]. This stage is observed throughout the belt, from the Ryuku Archipelago to the Boso Peninsula, as Middle Miocene terrains unconformably overlie deformed units from the Oligocene to the Early Miocene.

An earlier deformation stage is described in the Foliated Morotsuka, evidenced by isoclinal folds [*Sakai and Kanmera*, 1981] and by a N-S to NW-SE trending, stretching and mineral lineation associated to a top-to-the-N/NW sense of shear [*Charvet and Fabbri*, 1987; *Fabbri et al.*, 1987].

2.4. Metamorphism

Syndeformational metamorphic conditions (Table 1) have been determined from petrological analysis of slivers of oceanic basaltic material embedded within the different formations [*Imai et al.*, 1971; *Toriumi and Teruya*, 1988] as well as vitrinite reflectance [*Kondo et al.*, 2005] or illite cristallinity data in sedimentary rocks [*Hara and Kimura*, 2008; *Mukoyoshi et al.*, 2009]. The overall pattern is a decrease in the metamorphic grade from north to south, from prehnite-pumpellyite facies (~3–5 kbars for 200–300°C) in the Coherent Morotsuka to no significant metamorphic overprint in the Nichinan Group (Table 1). There is an anomaly in this general trend, as the highest grade unit is the Foliated Morotsuka/Foliated Kitagawa (300–310°C peak temperature [*Hara and Kimura*, 2008]), which is sandwiched between the slightly lower grade Coherent Morotsuka (i.e., 280–300°C) above and Hyuga Mélange below (i.e., 260–300°C).

Paleotemperature profiles show a rather smooth internal evolution within units but sharp changes across their limits. The largest discontinuity in the peak temperature profile occurs when crossing the NTL, with an ~50°C drop from the Foliated Morotsuka/Foliated Kitagawa into the Hyuga Mélange [*Hara and Kimura*, 2008]. Another smaller gap in paleotemperature defines the Oyabu Thrust, between the Hyuga Mélange and the Coherent Hyuga [*Hara and Kimura*, 2008]. In addition to the belt-perpendicular temperature variations, there is also a slight belt-parallel temperature gradient in the Hyuga Mélange, with temperature close to ~250°C to the east and ~280°C to the west [*Mukoyoshi et al.*, 2009].

2.5. Time Constraints on the Tectonometamorphic Evolution

Time markers for the tectonometamorphic evolution of the Shimanto Belt remain extremely fragmentary. In addition, the overall low metamorphic grade and the related scarcity of metamorphic minerals that can be unambiguously related to deformation limit the accurate distinction between crystallization, cooling, or deformation ages. The only available time constraints are summarized below and compiled in Table 1.

In the Foliated Kitagawa Group, *Mackenzie et al.* [1987] reported a single K-Ar age of 48.4 ± 1.1 Ma on recrystallized white mica composing the metamorphic foliation. In the Foliated Morotsuka Group, *Hara and Kimura* [2008] obtained two distinctive age sets on illite-rich fractions: Older Paleocene ages of 58.1 ± 2.9 and 54.9 ± 2.7 Ma and younger Eocene ages of 48.7 ± 2.4 and 49 ± 2.4 Ma. Combining these K-Ar ages with two additional fission track ages on zircon of 46.4 ± 2.6 (±1σ) and 47.9 ± 2.5 Ma, the authors propose to date the metamorphism in the Foliated Morotsuka as in the range of 46–50 Ma. On the other hand, zircon fission track datings along a NW-SE profile in Kyushu failed to give relevant results [*Hasebe and Tagami*, 2001]. Instead, peak *T* metamorphism of ~300°C, which fall within the zircon partial annealing zone (i.e., 230–330°C [*Tagami and Shimada*, 1996]), was not sufficient to reset fission tracks and then to enable to put accurate time constraints on the metamorphic stage. Conversely, apatite fission track analyses, dating the exhumation below the temperature range of ~75–125°C, gave consistent ages concentrated around 10 Ma in Cretaceous and Cenozoic units. The recent evolution of the belt is also constrained by a magmatism distributed throughout the Shimanto Belt, dated around 14 Ma [*Fabbri et al.*, 2004; *Shibata*, 1978; *Tanaka and Nozawa*, 1977], which cuts across earlier deformation structures such as the NTL [*Charvet and Fabbri*, 1987; *Letouzey and Kimura*, 1985; *Murata*, 1997].

Taken altogether, these results suggest the existence of (1) a common metamorphic stage for the Foliated Morotsuka and Foliated Kitagawa at approximately 46–50 Ma, i.e., in the early Middle Eocene and (2) a much more recent and widespread exhumation in Middle to Late Miocene, postdating all deformation stages in metamorphic context and uplifting the internal domains of the belt as well as the plutons cutting across them.

3. Deformation Analysis

To reconstruct the tectonic evolution of the Shimanto Belt, we describe the outcrop-scale deformation structures we collected along the coast and several rivers as follows: First, the attitude of the planar fabric is mapped in Figure 2, which is either the bedding stratification or the metamorphic foliation, depending on the formation considered and the amount of deformation. Ductile and brittle markers, from which we determined the kinematic directions, are shown in Figures 3 and 4. For ductile deformation, they correspond to the average trend of stretching lineation (Figure 3). Senses of shear in the ductile regime were determined according to indicators such as S-C fabrics or rotated objects, when present. For the

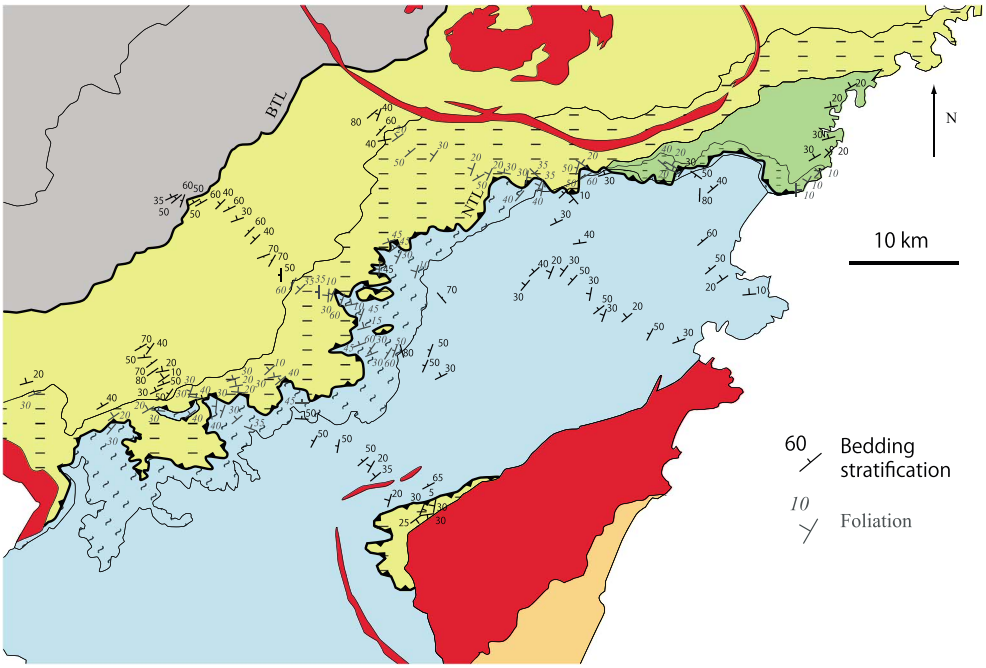

Figure 2. Map of the main planar fabric, corresponding to the bedding stratification in the Coherent Morotsuka, Coherent Kitagawa, and Coherent Hyuga and to a metamorphic foliation in the Foliated Morotsuka and the Hyuga Mélange. Bedding/foliation plane presents at the scale of the belt a NW dip. Dip angles are generally moderate to large except for the Foliated Morotsuka and the whole Kitagawa Group, where dip angle is smaller, on the order of 20°.

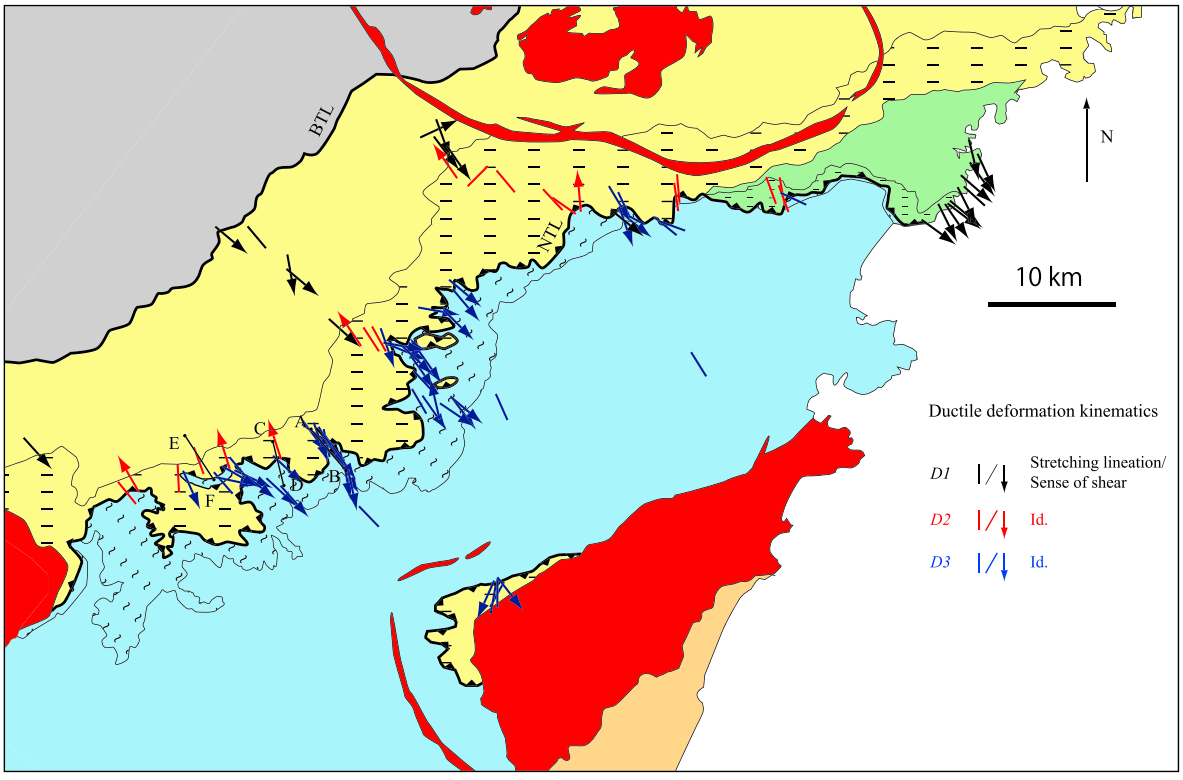

Figure 3. Ductile deformation map (see location in Figure 1). Nonarrowed rods indicate coaxial stretching; arrows indicate asymmetrical simple shear (e.g., arrows pointing to the north represent a top-to-the-north sense of shear). Deformation microstructures have been assigned to the tectonic stages defined in the text.

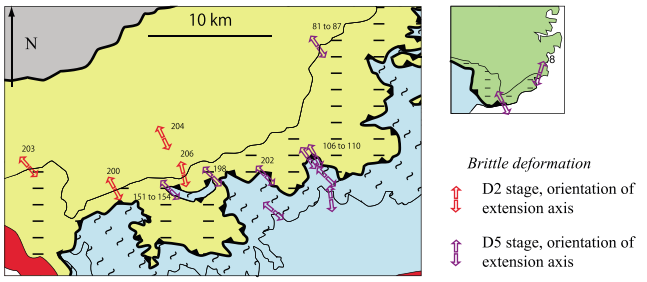

Figure 4. Brittle deformation map (see location in Figure 1). Double arrows represent the azimuth of the direction of extension. As explained in the text, brittle faults were associated with two distinct tectonic stages, D2 and D5.

brittle deformation, principal strain directions were determined by inversion of striated faults, or by averaging the strikes of fault *T* axes when inversion could not be performed (for example at sites where all the faults have similar strike, dip, and slickenside directions, such as normal fault dipping to the NW). Inversions and the average orientations of kinematic indicators were computed using Win_Tensor, a software developed by Damien Delvaux of the Royal Museum for Central Africa [*Delvaux and Sperner*, 2003]. Representative pictures of the deformation structures and their relative chronology are shown in Figures 5 to 8 and are summarized in Table 2. The organization of the field pictures follows the successive tectonic stages defined in section 4. Figures 9 and 10 incorporate cross sections and stereoplots representative of the deformation kinematics.

In the text that follows, to describe deformation structures, we have divided the whole belt into several domains, chosen either on the basis of stratigraphic ages or homogeneity of the tectonic style. For example, in spite of their different stratigraphic age (Cretaceous versus Early Eocene), the Morotsuka and Kitagawa Groups share the same large-scale structural division into a sandstone richer upper domain, where stratification bedding is mostly preserved (Coherent Morotsuka and Coherent Kitagawa) and a lower domain, more phyllite-rich, dominated by a flat-lying metamorphic foliation (Foliated Morotsuka and Foliated Kitagawa). For each domain, we describe the deformation structures and their kinematics, paying a particular attention, when it is possible, to the crosscutting relationship between sets of deformation markers.

3.1. Coherent Morotsuka and Coherent Kitagawa

The upper domain of the Morotsuka Group, the Coherent Morotsuka, is characterized by northward or northwestward dipping alternations of sandstone and mudstone in variable proportions, where most often stratification bedding is preserved. Most of the deformation is concentrated in relatively sparse ductile shear zones offsetting the sedimentary beds.

Part of deformation structures is related to the strong lithologic (i.e., rheological) layering of the sequence (Figures 5c and 5f) and locally by the presence of pillow lava slivers (Figures 5a and 5b). While thrusts generally develop as 30–50° dipping, layer-parallel surfaces in the sandstone layers, they conversely display a gentle to flat dips in the mudstone-rich layers (Figures 5d and 5e). These two types of faults, both oriented ~SW-NE to W-E, interact and often form flat-ramp-flat systems or sets of steeper reverse faults that bend down on a layer-parallel gently dipping master thrust fault. In parallel of these localized deformation structures, a more distributed deformation is present in the weak lithologies such as the mudstone-rich layers.

According to the lithological variations, the development of the stretching lineation is also highly dependent on the rheology of the material involved in the deformation. Sand-rich layers do not present any clear stretching direction. Conversely, conglomerate layers show a weak yet clear preferred orientation of the long axis of the clasts, while mudstone-rich layers present a conspicuous stretching lineation made of fine-grained phyllites such as chlorite, white micas, and coarser quartz grains. Stretching direction shows, consistently at the scale of the unit, a NW-SE trend (black rods/arrows in Figure 3).

At all scales, the ductile deformation within the upper domain of the Morotsuka Group is thus characterized by a general top-to-the-SE sense of shear, observed in the thrusts at the base of thick sandstone beds (Figure 5e), asymetrically boudinaged thin sandstone layers or basalt lenses (Figures 5a, 5c, and 5f) or distributed shear zones in the phyllite-rich layers (Figures 5b and 5d). The equivalent of this deformation can be found in the turbiditic, upper domain of the Kitagawa Group, described in detail by *Raimbourg et al.* [2009]: There, tens of meter-scale thrust faults and folds are associated with a stretching lineation, orientated NW-SE, on deformed quartz veins.

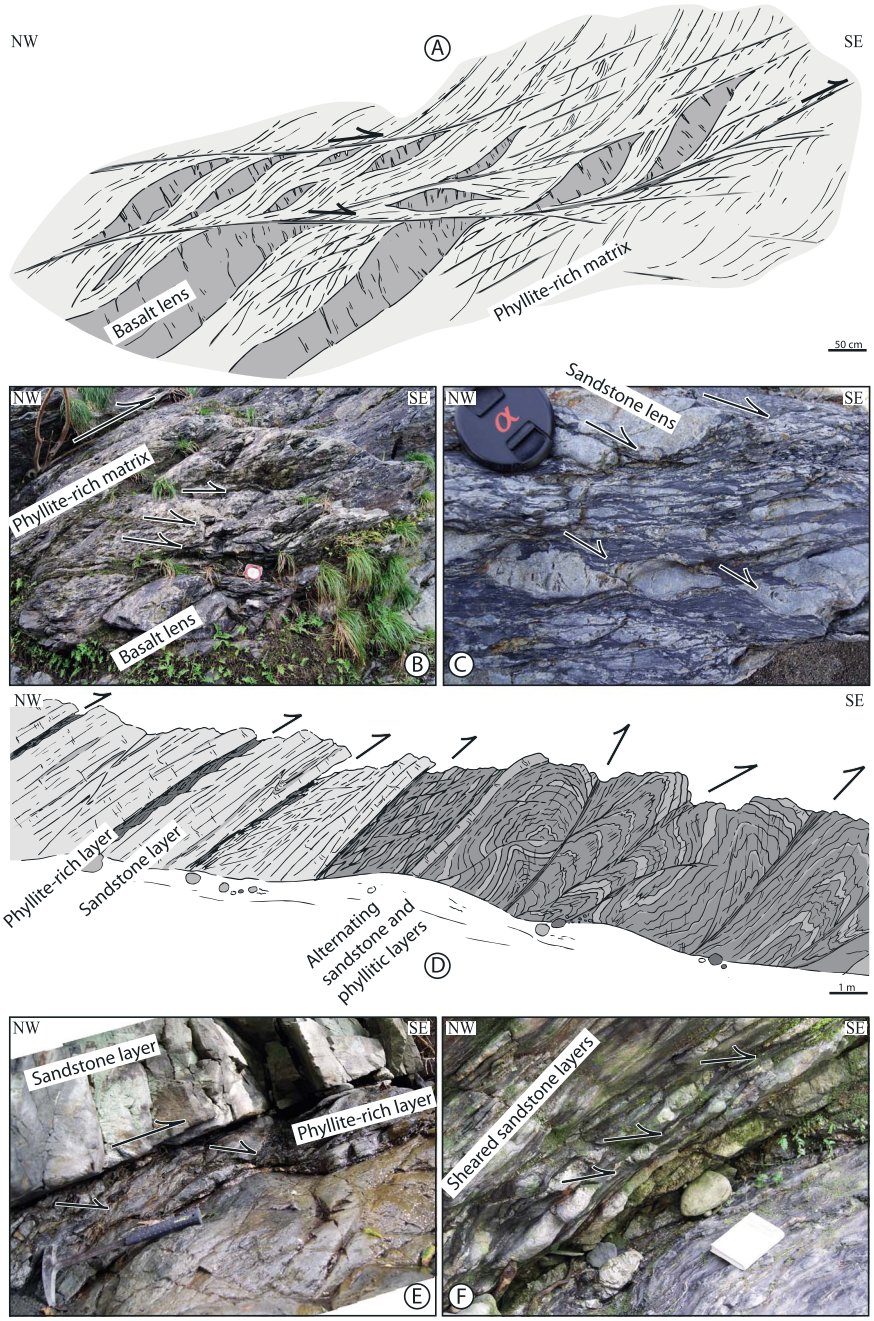

Figure 5. D1 deformation stage in the Coherent Morotsuka. (a and b) Basalt lenses embedded in a phyllite-rich matrix are asymmetrically sheared to the SE. (c and f) sandstone layers are cut by SE verging shear zones. (d) Cross section and (e) close-up view: The large top-to-the-SE shear zones run often parallel to thick, undeformed sandstone beds, while phyllite-rich beds are penetratively deformed by a dense network of gently dipping, smaller shear zones.

In addition to these ductile structures, brittle structures are also present in the Coherent Morotsuka. They mainly concentrate in the vicinity of thick sandstone beds (see cross section e-f in Figure 9) and in particular at the contact between the Coherent and Foliated Morotsuka (Figure 4, pink double arrows). Along the three cross sections where we could localize this limit, this contact is not the Tsukabaru Thrust, as indicated on the geological maps [*Saito et al.*, 1996; *Teraoka et al.*, 1990] but a dense array of striated normal faults distributed over a thickness of ~100–200 m. Some of these faults are made of a 1 to 20 cm-thick altered gouge (Figure 6e) and deflect significantly the foliation in the normal sense. The combination of these faults with adjacent small faults yields NNW-SSE direction of

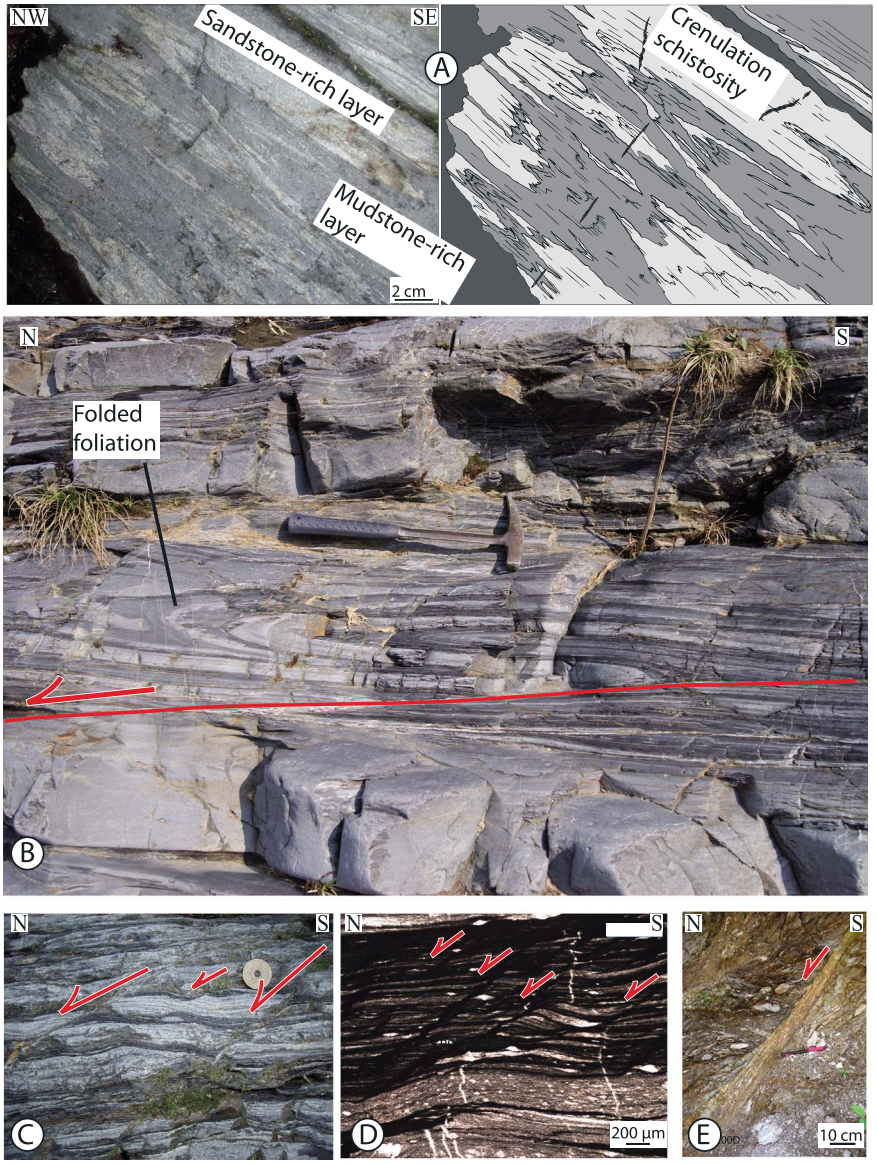

Figure 6. D2 deformation stage in the Foliated Morotsuka unit. (a and b) Strong vertical shortening/horizontal extension is apparent in isoclinal folds accompanied by the development of a fold axial planar foliation (=crenulation schistosity) principally composed of mica and quartz. (b, c, and d) Extension is locally asymmetric, with the top-to-the-NNW shear bands offsetting the metamorphic foliation and the folds. (e) Fault gouge, with the same top-to-the-NNW kinematics, localized at the limit between the Coherent and the Foliated Morotsuka.

extension (Sites 200, 203, 204, and 206 in Figure 10). We could not observe any clear chronology between ductile and brittle structures, as the former are particularly developed in phyllitic lithologies while the latter are mostly present in the vicinity of thick sandstone beds.

3.2. Foliated Morotsuka and Foliated Kitagawa

The lower structural domains of both Kitagawa and Morotsuka Groups, the Foliated Morotsuka and Foliated Kitagawa, share the same lithology (phyllite-rich with rare sandstone beds) and the same aspect of finely foliated rocks.

In contrast to the Coherent Morotsuka, where stratification bedding is still visible and deformation structures are relatively sparse, the Foliated Morotsuka, with a lithology richer in phyllites, was intensely deformed at ductile conditions, leading to the development of a ubiquitous metamorphic foliation with a

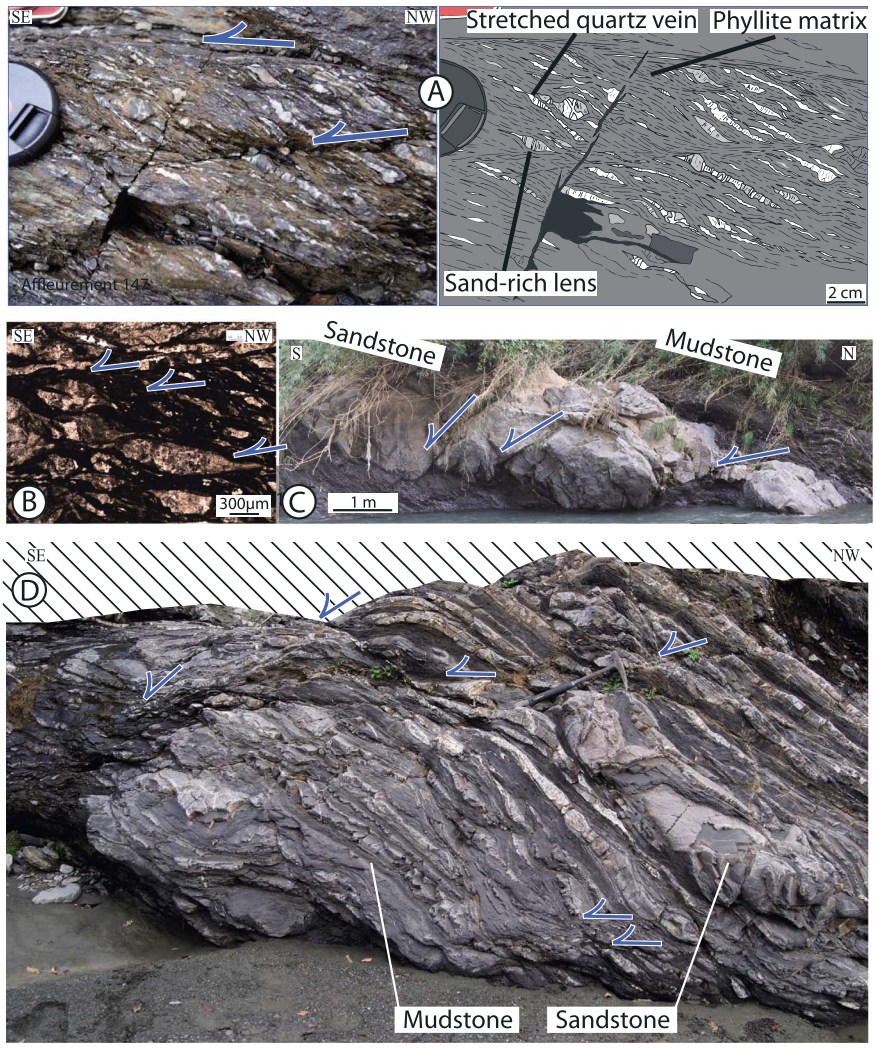

Figure 7. D3 deformation stage with the top-to-the-SE simple shear kinematics. (a and b) The top-to-the-SE shear zones, pervasive throughout the Hyuga Mélange unit, deform asymmetrically the centimeter- to millemeter-scale blocks of sandstones (light gray in Figure 7a, right) embedded in the phyllitic matrix (dark gray). Note the ubiquitous fragments of quartz veins (white), either cutting across sandstone blocks or as blocks in the matrix. (c and d) The top-to-the-SE faults and shear bands are also present in the structurally lower Coherent Hyuga, offsetting a large sandstone boudin surrounded by mudstone richer layers (Figure 7c) or alternating sandstone and mudstone beds (Figure 7d).

low (~20°) dip to the north (Figure 2). When it can be observed, the isoclinal folding affecting the Foliated Morotsuka at all scales (Figures 6a and 6b) shows that the foliation can be interpreted as a crenulation foliation. In the phyllite-rich domains, the discrimination between bedding and foliation is often not possible at the scale of the outcrop. At thin section scale, the foliation is defined by the preferential orientation of phyllosilicates (e.g., fine-grained white mica and chlorite), by the alternation of quartz-rich and phyllosilicate-rich layers and by elongated quartz veins. Simple shear criteria are particularly scarce, and the deformation is relatively coaxial. The foliation bears a stretching lineation made of preferentially orientated white micas and chlorite and orientated NNW-SSE (red rods/arrows in Figure 3).

In the Foliated Kitagawa, we observed a similar stage of deformation with the development of a subhorizontal foliation constituted principally of metamorphic chlorite and muscovite [*Raimbourg et al.*, 2009]. Magnetic fabrics determined by anisotropy of magnetic susceptibility showed that the strain ellipsoid is penny shaped (i.e., oblate type) without a clear stretching direction in its equatorial plane. This was confirmed in the field by the absence of a clear lineation in the foliation plane.

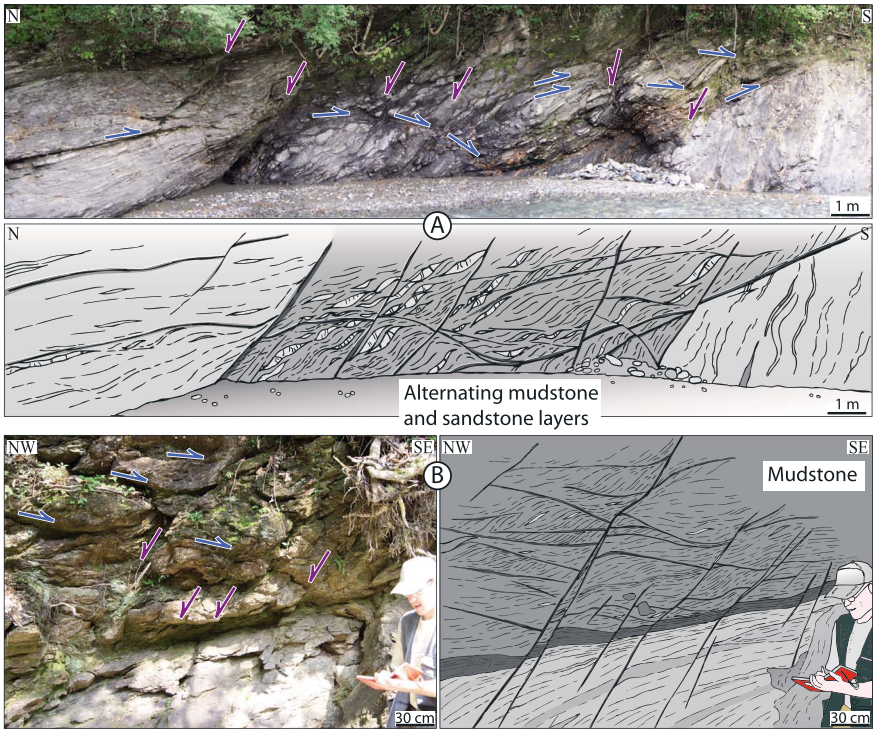

Figure 8. North or northwest dipping brittle faults (D5 stage). These faults offset D3, top-to-SE ductile shear zones ((a) Coherent Hyuga and (b) Hyuga Mélange) as well as earlier-stage thrusts such as the NTL.

In addition to the development of a metamorphic foliation, in the Foliated Morotsuka, small ductile shear bands locally cut the foliation at low angle. Some of these shear bands show a top-to-the-NNW sense of shear (Figures 6c and 6d) that cannot be found in any other formation of either the Cretaceous or Cenozoic Shimanto, while others show a top-to-the-SE sense of shear. In most instances, depending on the cross section considered, either top-to-the-SE or top-to-the-NNW shear bands dominate (e.g., Site 203 or Site 106 for top-to-SE movement, Site 200 or Site 202 for top-to-NNW, Figure 10), and only in one case, they coexist and seem to be synchronous (Sites 151 and 152).

Finally, normal faults, with a large (~50–60°) dip to the NW and NW-SE direction of extension, are rarely present and offset the shear bands.

3.3. Hyuga Mélange

The Hyuga Mélange unit is the most strongly deformed unit of the whole Shimanto Belt on Kyushu. The typical Mélange facies are made of a finely foliated, phyllite-rich matrix, enclosing blocks of various sizes from millimeter to decimeter. The foliation is defined by the preferential orientation of chlorite and flattened blocks made of either pinched sandstone beds or boudinaged quartz veins (Figures 7a and 7b). A consistent feature of the Hyuga Mélange is the density of quartz veins, which affect principally the sandstone blocks. These veins sometimes present plastic deformation and are parallelized to the foliation.

The foliation presents a general gentle to moderate dip to the north (30–40°) (Figure 2). Stretching, defined by elongated sandstone blocks and quartz veins, is NW-SE (blue rods/arrows in Figure 3). The deformation is strongly noncoaxial, as attested by pervasive networks of shear zones, composed of quartz and chlorite with a composition similar to foliation-forming one. These shear zones have a very variable lateral extent, from a few centimeters up to a few meters, and dip either to the NW or to the SE (Figures 9 and 10), with a very low angle (0–15°). Sigmoids of matrix foliation or blocks along these bands indicate a dominant top-to-the-SE sense of shear (Figures 7a and 7b and blue arrows in Figure 3), even if some restricted areas show the coeval development of conjugate sets of shear bands (blue rods in Figure 3).

Ductile structures, including foliation and top-to-the-SE shear bands, are crosscut by striated normal fault planes dipping at ~50° to the NW or N (Figures 8a and 8b), compatible with a NW-SE extension

AGU Tectonics

10.1002/2013TC003412

Table 2. Distribution, Into the Five Tectonic Stages, of the Deformation Structures Described in the Different Units[a]

Unit	Contacts	D1	D2	D3	D4	D5
Coherent Morotsuka		Rare top-to-the-SE shear bands	*NNW dipping faults with NNW-SSE extension, localized near thick sandstone beds*			
	100-200m thick zone		***NNW dipping faults with NNW-SSE extension***			
Foliated Morotsuka			Flat-lying metamorphic foliation, locally axial planar to isoclinal folds Top-to-the-NNW shear zones			*Rare NW dipping faults with NW-SE extension*
Coherent Kitagawa		Stretched quartz veins *Top-to-the-SE faults and folds*				*Rare NW dipping faults with NW-SE extension*
Foliated Kitagawa			Flat-lying metamorphic foliation, no clear stretching lineation			*Rare NW dipping faults with NW-SE extension*
	Nobeoka Tectonic Line				***10cm thick cataclasite, with top-to-the-SE transport***	***NW dipping faults with NW-SE extension***
Hyuga Mélange				Top-to-the-SE, pervasive shear bands		*NW dipping faults with NW-SE extension*
	Oyabu Thrust (?)				**?**	***NW dipping faults with NW-SE extension***
Coherent Hyuga				Rare top-to-the-SE shear bands		*Rare NW dipping faults with NW-SE extension*

[a]Regular/*Italic* characters refer to ductile/*brittle* structures. The column "contacts" corresponds to the limit between a unit and the one following in the list, and the corresponding structures are in bold. Note that in place of the Oyabu Thrust, described by *Hara and Kimura* [2008], we found only normal faults. The top-to-the-SE shear zones in the Foliated Morotsuka are not shown in the table as we could not determine their timing.

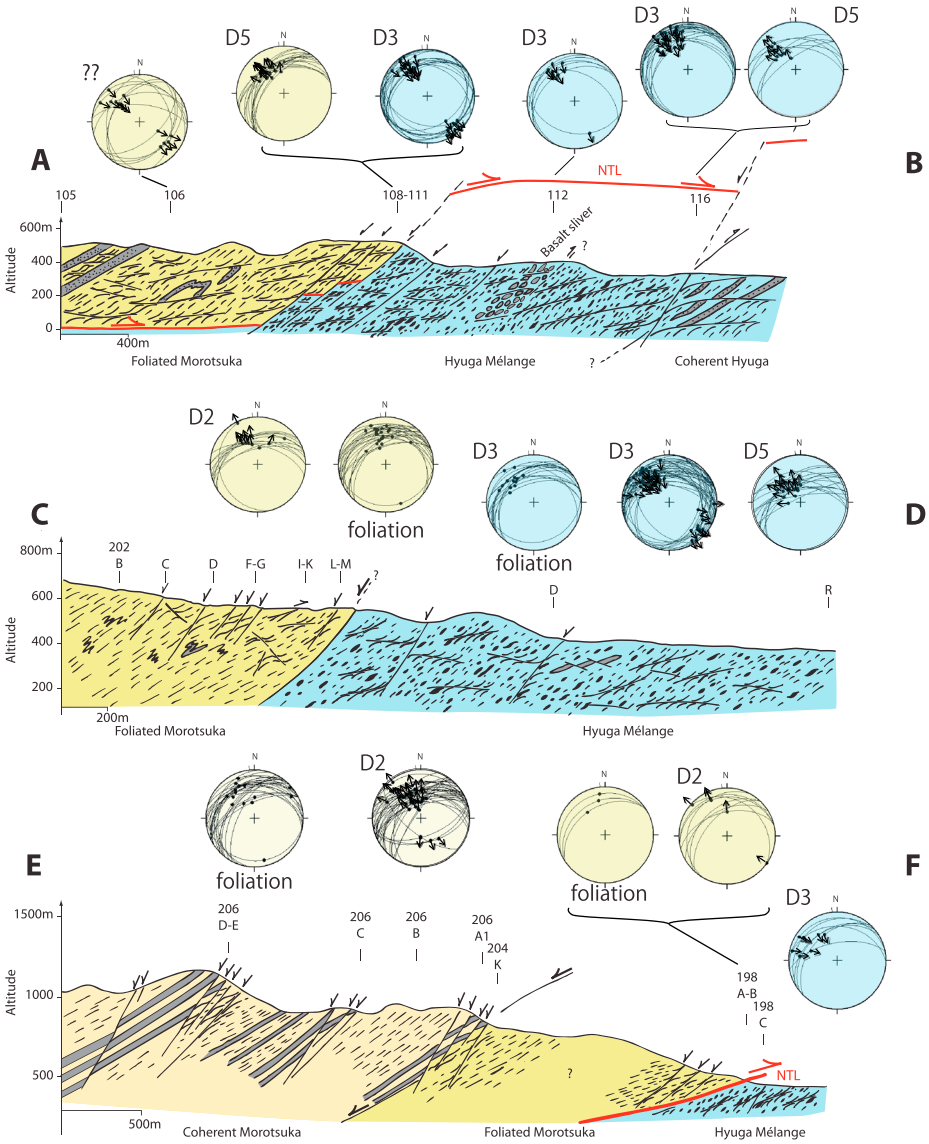

Figure 9. Cross sections through the Morotsuka and Hyuga Groups (see location in Figure 3 and outcrop references in Figure 4). (a-b) The dominant ductile deformation in the Foliated Morotsuka and the Hyuga Mélange is the top-to-the-SE shear. The NTL is interpreted as an out-of-sequence thrust postdating ductile deformation. All present contacts (Morotsuka-Hyuga Mélange and Hyuga Mélange-Coherent Hyuga) result from an extension accommodated by normal faults of stage D5. (c-d) Folded sandstone beds in Morotsuka units illustrate the foliation-perpendicular D2 stage of deformation accompanied by the top-to-the-NNW shear bands. The top-to-the-SE ductile deformation of D3 stage is pervasive in Hyuga Mélange and is crosscut by late-stage D5 faults. The contact between Foliated Morotsuka and Hyuga Mélange could not be observed in this cross section. (e-f) D2 stage deformation is localized principally at the contact between Foliated and Coherent Morotsuka as an ~100 m thick zone of extensional deformation including numerous ~1–30 cm thick brecciated gouges. Similar zones of concentrated extensional deformation are localized in the vicinity of massive sandstone beds in Coherent Morotsuka and near the NTL. Note the slight obliquity between the NNW-SSE directions of D2 faults and NW-SE direction of D3 deformation in underlying Hyuga Mélange. Stereoplots in all sections as lower hemisphere, equal area projections. Pale yellow/bright yellow/blue plots refer to Coherent Morotsuka/Foliated Morotsuka/Hyuga Mélange, respectively. For faults and shear zones, arrows indicate the relative movement of the hanging wall unit along the lineation/striation. No vertical exaggeration.

under brittle conditions (Figures 4, 9, and 10). These faults are sparsely distributed within the whole Hyuga Mélange and concentrated near the upper (NTL) or lower boundary of the formation. Along cross sections (a-b in Figure 9), the contact between the Foliated Morotsuka and the Hyuga Mélange is marked by a few tens of meters-thick zone characterized by a dense network of normal faults. Farther

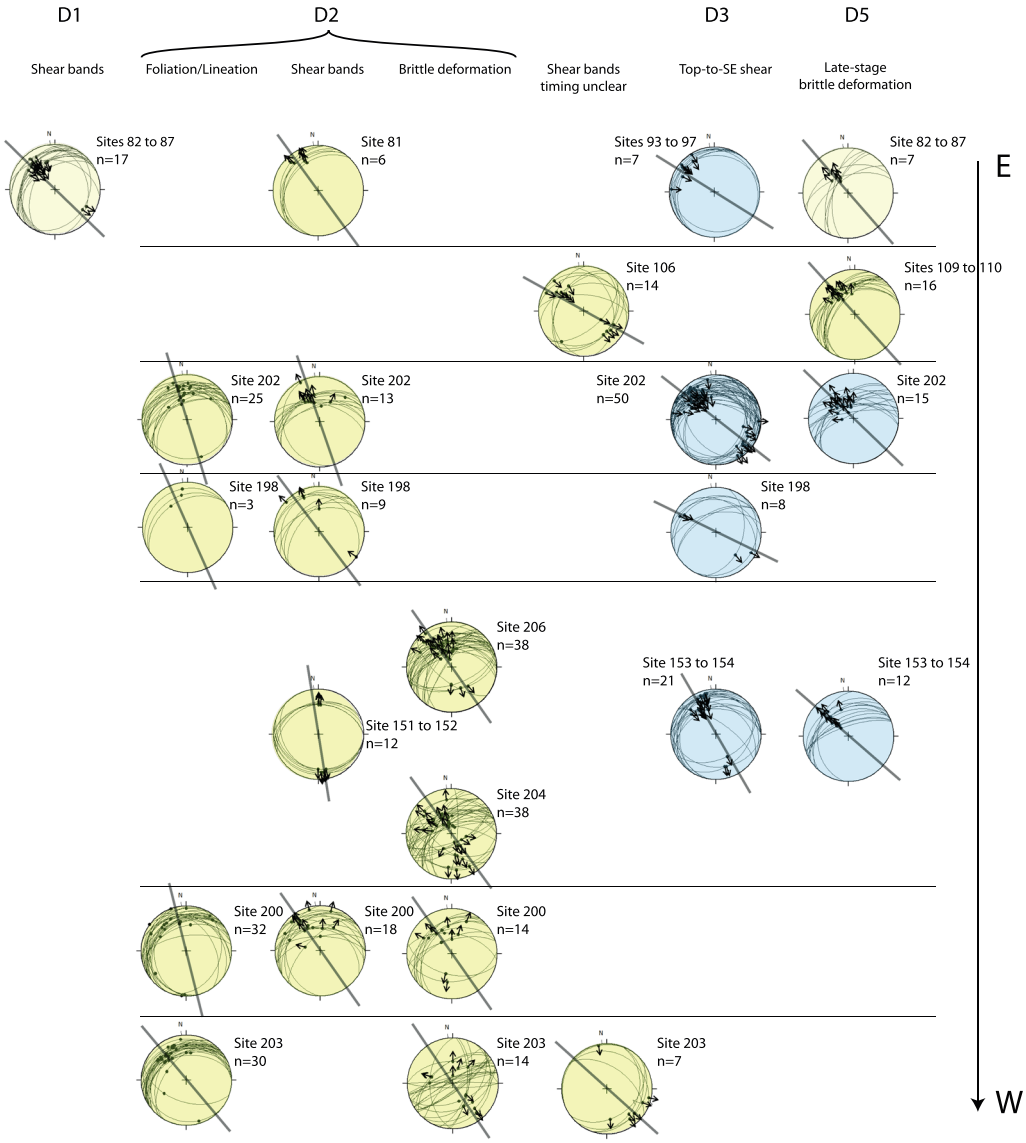

Figure 10. Representative equal area, lower hemisphere, stereographic plots of deformation stages: Each line corresponds to a cross section along a river, distributed from east to west moving downward in the figure. Pale yellow/bright yellow/blue plots refer to Coherent Morotsuka/Foliated Morotsuka/Hyuga Mélange, respectively. Note that the timing of the top-to-the-SE shear in Foliated Morotsuka is unclear (see text).

downstream along the same cross section, the contact between Hyuga Mélange and Coherent Hyuga is a sharp fault steeply dipping to the north, although no striation has been found. Along the coast near Nobeoka City, the NTL, which makes the contact between the Foliated Kitagawa and the Hyuga Mélange, is crosscut by several normal faults dipping to the SE, giving a similar NW-SE direction of extension (Figure 4).

3.4. Coherent Hyuga

Below the Mélange, the rest of the Hyuga Group is much similar to the Coherent Morotsuka: It is mostly made of alternating sandstone-rich and mudstone-rich formations, where in most instances, turbidite beds of various thickness are still preserved. Faults and shear bands are absent from most outcrops. When present, shear zones cut across and offset the stratification bedding (Figures 7c and 7d), with a top-to-the-SE shear sense.

4. Deformation Stages

4.1. Structural and Time Constraints on the Tectonic Stages

The structural observations described above can be synthetized as follows:

1. Deformation structures are dominated by the top-to-the-SE shear zones. There is no clear time constraint on these structures, and they are distributed over zones of various stratigraphic ages, from Cretaceous terranes in the Morotsuka Group to the Oligocene terranes of the Coherent Hyuga.
2. Two distinct sets of microstructures contrast with the top-to-the-SE kinematics: First, a flat-lying foliation is developed in Foliated Morotsuka and Foliated Kitagawa, in some places planar axial to small-scale isoclinal folds. Second, top-to-the-N or NW structures are well developed into the Foliated Morotsuka and in the Hyuga Mélange. In the Foliated Morotsuka, they consist in top-to-the-N or NW, (i) distributed shear zones and (ii) faults localized along the formation upper boundary. In the Hyuga Mélange, the top-to-the-NW faults are distributed in the formation and concentrated around its lower and upper boundaries. The faults in the Hyuga Mélange cut across the top-to-the-SE shear zones and across the NTL, as can be seen in its exposure along the coast.

As a result, from our structural analysis, only a single temporal constraint clearly emerges: There is a late stage of extension, characterized by the top-to-the-NW faults, which postdates the ductile deformation in the Hyuga Mélange and the movement on the NTL.

At this point, an additional constraint can be put forward: The age of the metamorphic foliation is estimated by K-Ar ages on illite and zircon fission track dating at ~48 Ma, i.e., in early Middle Eocene, both in the Foliated Morotsuka [*Hara and Kimura*, 2008] and the Foliated Kitagawa [*Mackenzie et al.*, 1990], while the youngest biostratigraphic ages of Hyuga Mélange fall at the end of the Middle Eocene, at ~37 Ma in *Sakai et al.* [1984]. The development of the metamorphic foliation in early Middle Eocene in the Foliated Morotsuka and in the Foliated Kitagawa necessarily predates the top-to-the-SE ductile deformation recorded in the Hyuga Mélange.

4.2. Definition of the Tectonic Stages

The combination of structural and age data leads therefore to distinguish three successive stages of deformation: (a) development of a foliation in early Middle Eocene in the Foliated Morotsuka and Foliated Kitagawa, (b) top-to-the-SE ductile deformation in the Hyuga Mélange, and (c) NW-SE brittle extension in the Mélange, without precise dating of the last two stages.

We can now speculate on this relatively robust time sequence to determine the timing of all the top-to-the-SE structures collected on the field: Do they relate to a single, temporally limited event or are these deformation structures diachronously recorded in the various units?

Geometrically, the top-to-the-SE shear is consistent, both in terms of direction and sense of shear, with the dynamics of the modern margin, where material is accreted either at the front or below the prism. One can imagine therefore that the top-to-the-SE deformation results from accretion; hence, the top-to-the-SE structures are only slightly younger than the biostratigraphic terranes they affect and they formed diachronously as the Shimanto Belt grew from late Cenozoic to the present. This is the dominant model of the Shimanto Belt as a giant accretionary prism [*Taira et al.*, 1988], where the dynamics of the modern margin apply to the whole evolution of the belt. If we follow such model, then the top-to-the-SE deformation recorded in the Coherent Morotsuka closely follows its accretion in Cretaceous, hence constitutes a deformation stage predating the metamorphic event in early Middle Eocene (Table 1). This is confirmed on the eastern coast, in the Foliated Kitagawa, where the metamorphic event in early Middle Eocene is superimposed on an early-stage, accretion-related deformation characterized by large-scale thrusts offsetting folded turbidite beds with a top-to-the-SE kinematics (Figure 3 in *Raimbourg et al.* [2009]).

Another question is the relationships between the pervasive, top-to-the-SE ductile deformation in the Hyuga Mélange and the highly localized movement on the NTL, which have similar kinematics [*Kondo et al.*, 2005]. One possibility is that Mélange deformation is associated with the movement on the NTL. The best argument against the latter hypothesis lies in the spatial relationship between the NTL and the deformation within the Hyuga Mélange: In the eastern side of Figure 1, the NTL is cutting across the contact between the Hyuga Mélange and the Coherent Hyuga. In the Mélange, the deformation is pervasive, whereas it is much more limited in the Coherent Hyuga, even just underneath the NTL. This shows that the deformation localized in

the Mélange in the west of the map predates the initiation of the NTL. Consequently, the movement on the NTL is a distinct, younger event, which hardly affects both the hanging wall and the footwall in spite of the tens of kilometers of transport.

As a result, we propose to distinguish five stages of deformation (Table 2):

D1: Diachronous and earliest stage of deformation, apparent in the top-to-the-SE shear zones of the Coherent Morotsuka and Coherent Kitagawa. The mechanism of deformation is probably frontal accretion: these units contain thick turbidites beds and correspond therefore to the upper part of a typical sedimentary sequence incoming at the trench, which is to a large extent incorporated to the prism through the propagation of in-sequence, frontal thrusts. In addition, the shear zones observed in these units are geometrically similar to frontal thrusts. A further argument in favor of frontal accretion, a shallow process, is the absence of clear metamorphic minerals in the shear zones.

D2: Development of a flat-lying metamorphic foliation as a result of vertical shortening, in early Middle Eocene, coeval with peak metamorphic conditions, affecting the Foliated Morotsuka and Foliated Kitagawa.

D3: Top-to-the-SE shear concentrated in the Hyuga Mélange. The Hyuga Mélange pervasive simple shear fabrics and block boudinaging is a relatively deep deformation, as it involves chlorite shear zones and quartz veining and shearing (Figures 7a and 7b). Consequently, we propose to interpret Hyuga Mélange deformation as the result of shearing during subduction and underplating, similarly to what is commonly observed in exhumed tectonic mélanges [*Byrne and Fisher*, 1990; *Kimura and Mukai*, 1991; *Onishi et?al.*, 2001]. In the hypothesis of underplating, the deformation age would be younger than, but probably close to, Mélange youngest stratigraphic ages, hence Late Eocene to Early Oligocene [*Sakai et?al.*, 1984].

D4: Formation of and top-to-the-SE movement on the NTL.

D5: NW-SE, late-stage extension through normal faults. Some of these faults are distributed in the Hyuga Mélange; some cut across earlier thrust contacts between units such as the NTL.

4.3. Interpretation of the D2 Stage

The D2 stage stands at variance with the usual dynamics of accretionary prism and needs therefore further discussion, first concerning the microstructures related to it and second its large-scale significance.

In addition to the dominant flat-lying metamorphic foliation, various noncoaxial deformation microstructures were locally observed in the Foliated Morotsuka (e.g., shear zones with opposite vergence and brittle faults along the northern boundary). In most cross sections, only one vergence of shear zone dominates (e.g., Site 203 or Site 106 for the top-to-SE movement, Site 200 or Site 202 for the top-to-NNW, Figure 10), and only in one case, they coexist (Sites 151 and 152), which makes it difficult to analyze the temporal relationships of the opposite vergence shear zones.

There are several arguments to connect the top-to-the-NNW shear zones to the D2 stage: (i) the occurrence of these shear zones is restricted to the Foliated Morotsuka, such as is restricted the metamorphic foliation related to D2 (but for the similar lower domain of the Kitagawa Group along the coast), and (ii) there is an obliquity between the direction of the top-to-the-NNW shear zones and the top-to-the-SE kinematics of the D3 stage, visible in the observations made on Sites 198–206 (cross section e-f in Figure 9) and Site 202 (cross section c-d in Figure 9). There, (i) in the Foliated Morotsuka Group, the top-to-the-NNW shear direction is roughly parallel to lineation on the foliation, and (ii) this direction (NNW-SSE) is oblique to the direction of the top-to-the-SE shear recorded in underlying Hyuga Mélange, corresponding to the D3 stage.

The same argument holds for the faults in the Coherent Morotsuka, which yield an NNW extension slightly oblique with respect to the extension obtained by the inversion of late-stage faults in the Hyuga Mélange, directed rather NW-SE (see for example Site 206 versus Site 198 in Figure 4). In addition, the offset on these faults is responsible for the anomalous metamorphic gap, visible in vitrinite reflectance-derived temperatures [*Hara and Kimura*, 2008], across the limit between Coherent and Foliated Morotsuka. Unlike all other contacts, even those reworked by the late-stage normal faults in the Mélange, the grade of the structurally upper unit is lower than that of the lower unit. We propose therefore that the brittle faults in the Coherent Morotsuka, with a direction of extension NNW-SSE, were formed during the D2 stage, similarly to the top-to-the-NNW ductile shear zones. The coexistence during the D2 stage of the ductile shear zones and brittle faults can be explained in two ways: (1) ductile shear zones are in a structurally

lower position than faults, with a slight temperature difference apparent in vitrinite reflectance [*Hara and Kimura*, 2008] and (2) faults are associated with thick sandstone beds, while ductile shear zone are pervasively distributed in more pelitic material.

In contrast, the relation between the top-to-the-SE shear zones in the Foliated Morotsuka and the D2 stage is not clear, although they might be contemporaneous.

As a result, the metamorphic event in the Foliated Morotsuka can therefore be interpreted kinematically as dominantly coaxial, subvertical shortening, leading to the development of isoclinal folds and a subhorizontal, metamorphic crenulation foliation, with a minor contribution of heterogeneously distributed shear bands. There might be a noncoaxial component in the deformation, resulting from the predominance of the top-to-the-NNW shear bands and faults over the top-to-the-SE shear bands, but this point is still unclear as the timing of the latter shear zones is not well constrained. In the Foliated Kitagawa, the kinematics of the D2 stage is much simpler, as no shear bands were observed and only the development of the flat-lying foliation and the vertical shortening of passive markers such as quartz veins is apparent, without a clear stretching direction [*Raimbourg et al.*, 2009].

The interpretation of the flat-lying foliation, with subvertical shortening, is not straightforward in the general context of accretionary prisms, dominated by simple shear deformation. One possibility is that the flattened Foliated Morotsuka and Foliated Kitagawa are rotated domains of pure shear subsidiary to master shear zones limiting them. In such case, the large-scale kinematics would not be pure shear, as apparent at outcrop scale, but simple shear. In other words, the pure shear deformation observed on the field would be a local phenomenon in a large-scale pattern of simple shear deformation.

We discard this hypothesis as we could not find any evidence for such large-scale shear zones within or along the upper and lower boundaries of the Foliated Morotsuka or Foliated Kitagawa. This absence is most undisputable in the Foliated Kitagawa, which crops out continuously along the eastern coast of Kyushu. Shear zones, whatever their vergence, are invariably small-scale objects subsidiary to the main foliation, and no master shear zone is present. We therefore propose that the kinematics leading to the formation of the foliation by dominant vertical shortening is valid not only at the outcrop scale but also at the kilometer scale, i.e., at the scale of the domains that are affected by this foliation.

In summary, the D2 stage results from vertical shortening/horizontal extension. It is apparent as a widely distributed ductile deformation in the Foliated Morotsuka and Foliated Kitagawa. It is much more discrete in the structurally above and sandstone-rich units of Coherent Kitagawa and Coherent Morotsuka, as only rare zones of concentrated brittle faults in the Coherent Morotsuka are possibly associated to it. The geodynamical and mechanical interpretation of the D2 stage and its kinematics are discussed in the following reconstructions of the belt.

5. Reconstruction of Shimanto Belt Evolution

For these reconstructions (Figure 11), we have considered a continuous subduction of an oceanic plate below SW Japan. Starting from the present-day geometry of the Shimanto Belt, we have reconstructed backward its evolution with the constraints of (1) balance of the domains of the belt with different ages, (2) deformation kinematics of the five stages, (3) sedimentological facies of the various units, and (4) metamorphic constraints on peak burial conditions reached by several material points used as passive markers. Note that the latter requirement is rather imprecise, as, except for *Toriumi and Teruya* [1988], where paleopressure estimates of Hyuga Mélange are provided, for most formations, only paleotemperatures are known [*Hara and Kimura*, 2008], which can hardly be converted into paleodepths in the context of ridge subduction described below and where geothermal gradients have probably changed a lot with time. For the accretion, we have also followed models of modern margins, where the growth of the prism results from both frontal accretion (i.e., mostly for the trench-filling sediments on top of the incoming sedimentary sequences) and underplating at depth (for deeper facies sediments above the subducting oceanic crust).

5.1. Situation During the Paleocene

During the Paleocene, the Shimanto Belt is composed of an inner domain of accreted Cretaceous terranes and an outer domain of accreted Paleocene terranes. The Cretaceous belt is oversimplified. Stratigraphic age gaps of the northern Shimanto Belt indicate the existence of two diachronous subbelts [*Teraoka et al.*, 1994], the Saiki

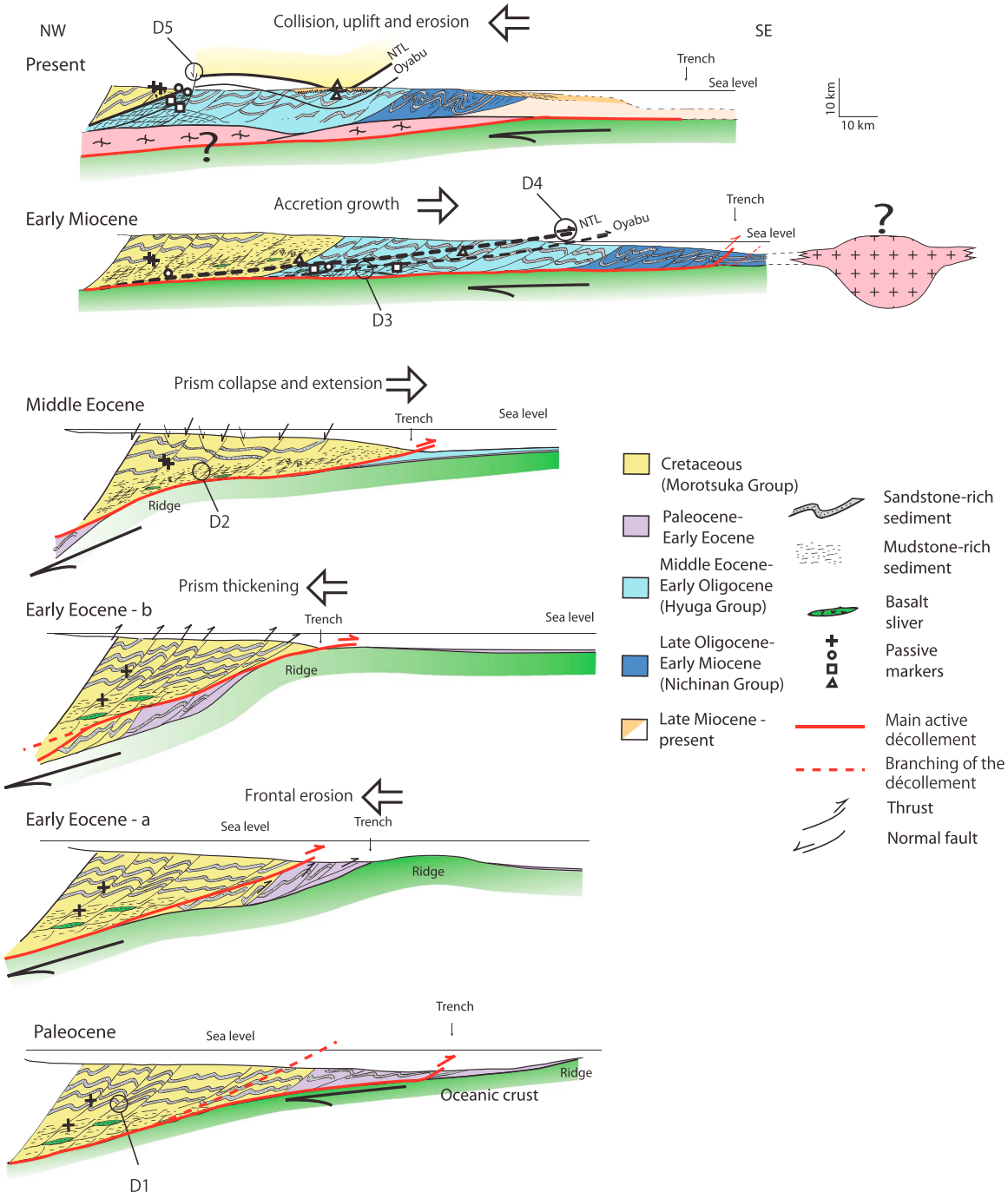

Figure 11. Geodynamical evolution scheme integrating the deformation features observed on the field as well as stratigraphic constraints. Crosses, triangles, and circles are particles passively transported during deformation and now in contact in present stage. "D1" to "D5" refer to the tectonic structures/stages discussed in the text. Paleocene: The accretionary prism is constituted of underplated, phyllite-rich slivers at depth and sandstone richer units near the surface. Due to the lack of structural data, note that the internal structure of the wedge is oversimplistic with respect to stratigraphic age constraints [*Teraoka et al.*, 1994]. Early Eocene a and Early Eocene b: Ridge subduction triggers the thickening of the prism and the erosion of its frontal part, of Paleocene/Early Eocene age, dragged into subduction. Middle Eocene: After ridge subduction, the whole prism collapses and extends through normal faulting near the surface and ductile extension at depth, corresponding to the D2 stage recorded principally in the Foliated Morotsuka and the Foliated Kitagawa. Early Miocene: Accretion of the Mélange by underplating (D3 tectonic stage) and very rapid growth by frontal accretion of the whole Hyuga Group prism occur in Late Eocene and Early Oligocene. A repeated stage of rapid accretion leads to addition of the Nichinan Group in Early Miocene. The NTL and associated low-angle thrusts, to be activated during subsequent collision stage (Takachiho phase–D4 stage), appear as dashed lines. A possible cause for this collisional stage is shown as a small continental block on the lower plate. Present: During the Takachiho phase, the accretionary prism is horizontally shortened, and large-scale, low-angle thrusts are activated before being folded. A late-stage extension (D5 stage) results in normal faults offsetting earlier deformation structures such as thrust contacts.

and Kamae Subbelts, from north to south. According to these authors, the Foliated Morotsuka (named Kamae Subbelt there) is the youngest subbelt, with limited age overlapping with the more sandstone-rich, overlying Coherent Morotsuka (named Saiki Subbelts there), so that the two subbelts cannot originate from a single lithostratigraphic section and have to be diachronously accreted. Due to the lack of additional information, we did not show this stage of accretion and represented only the Cretaceous formations in their present-day structural position, with the sandstone-rich Coherent Morotsuka overlying the Foliated Morotsuka.

5.2. Early Cenozoic Deformation: Effects of a Ridge Subduction on the Margin

Summarizing, the early Cenozoic tectonic stage has to explain simultaneously: (1) a phase of extension described in the Shimanto Belt on Kyushu and dated around 48 Ma and (2) a change in the direction of convergence recorded both on Kyushu (this work) and on Shikoku [*Byrne and DiTullio*, 1992; *Lewis and Byrne*, 2001], dated in the Eocene.

While classical paleogeographic reconstructions predict that the Kula-Pacific Ridge swept the SW Japan Trench in late Cretaceous [*Engebretson et al.*, 1985], new reconstructions, based on the assumptions of symmetrical and steady spreading rate of the Izanagi-Pacific Ridge [*Whittaker et al.*, 2007], describe a different scenario, more compatible with the geological facts listed above.

In the reconstructions by *Faccenna et al.* [2012], *Müller et al.* [2008], and *Whittaker et al.* [2007], the Izanagi-Pacific Ridge, trending almost parallel to the Japanese margin, arrived at the trench at 60 to 55 Ma. One of the consequence of this ridge subduction is a large-scale reorganization of plate dynamics in the whole Pacific area [*Müller et al.*, 2008], including a counterclockwise rotation by ~45° of the convergence direction between Izanagi/Pacific and Eurasia around 50 Ma [*Faccenna et al.*, 2012; *Whittaker et al.*, 2007]. This change in convergence nicely mimicks the change in the kinematic directions observed in the Shimanto Belt. Ridge subduction, with associated thermal overprint, can also explain the abnormal paleothermal structure of the Cretaceous Shimanto, as was also proposed by *Sakaguchi* [1999].

The D2 stage, anomalous with respect to the usual dynamics of accretionary prisms, is therefore coeval with an anomalous event during oceanic subduction: the subduction of a trench-parallel ridge. The effect of a ridge subduction on the dynamics of the overlying prism is far from clear, and there are several possible models to connect the ridge subduction to the peculiar extensional kinematics of the D2 stage:

1. Underplating: Following *Platt*'s [1986] model, in case of underplating, horizontal extension of the wedge is required to maintain a constant taper angle. The link between ridge subduction and enhanced underplating is nevertheless not clear: As the ridge sediment cover is thin, enhanced underplating during ridge subduction would require that the ridge itself, or slices of oceanic crust, are underplated. This is contradictory to the geological record, which does not show that an anomalously large volume of Paleocene or Early Eocene oceanic crust was incorporated to the Shimanto Belt [e.g., *Taira et al.*, 1988].
2. Slab breakoff: The scenario by *Müller et al.* [2008] includes slab breakoff as a result of ridge subduction. Note that the slab breakoff theory is not taken over by *Faccenna et al.* [2012], and the convergence velocity is hardly affected by the ridge subduction. The mechanical consequences of slab breakoff on the overlying accretionary prism are currently not known. In the model of *Von Blanckenburg and Davies* [1995], which focuses on continental subduction in the Alps, there is a strong effect of slab breakoff on magmatism, but the tectonic consequence is mostly restricted to the uplift of deeply subducted rocks along the subduction plane. The mechanical effect of slab breakoff on deformation regime in the overlying plate is not elucidated.
3. Thickening, then erosion, and collapse of the accretionary prism: Analog modeling of seamount subduction have shown that in front (i.e., landward) of the seamount, the accretionary prism is strongly shortened and uplifted through the reactivation or the formation of thrusts [*Dominguez et al.*, 1998, 2000; *Lallemand et al.*, 1992]. The deformation in the trail of the seamount is less clear: In some experiments, renewed accretion through thrusting closely follows the seamount subduction [*Dominguez et al.*, 2000], while other experiments show extension in the seamount wake, with the development of a set of landward dipping normal faults [*Dominguez et al.*, 1998]. Natural examples of trench oblique ridge or seamount subduction show that the subducting topography may also erode the overlying prism and drag down slices of it [*Bangs et al.*, 2006]. The consequence of basal erosion on the accretionary prism is the formation of normal faults, as is observed along the Ecuador convergent margin [*Sage et al.*, 2006]. Extension in the accretionary wedge, as evidenced by normal faulting, is a consistent feature of erosive margin such as Japan or Peru [*Von Huene and Lallemand*, 1990].

The scenario of a subducting ridge triggering erosion then collapse of the overlying accretionary prism provides therefore a mechanical model to account for the extension recorded during the D2 stage.

As a result, the scenario chosen in the reconstructions (Figure 11) involves the following main stages:

1. Subduction of the oceanic Izanagi Plate during Paleocene below a growing accretionary prism (Figure 11 "Paleocene")).
2. In Early Eocene, onset of Izanagi-Pacific Ridge subduction with similar effects to seamounts indenting the margins, triggering thickening of the prism, erosion of its frontal portion [*Bangs et al.*, 2006; *Von Huene and Lallemand*, 1990], and dragging down of the Paleocene and early Eocene terranes, consistent with their scarcity in the Shimanto Belt (Figure 11 "Early Eocene a" and "Early Eocene b").
3. Subsequently to the ridge subduction and erosion of the margin, collapse of the prism with normal faulting in the shallower part and ductile extension in the deeper part of the wedge (Figure 11 "Middle Eocene"). The D2 stage is the geological record of such extension, mostly apparent in the Foliated Morotsuka and the Foliated Kitagawa and possibly through landward dipping normal faults in the Coherent Morotsuka.

5.3. Deformation and Accretion From the Late Eocene to the Miocene

5.3.1. Rapid Wedge Growth in the Late Eocene-Miocene

5.3.1.1. Hyuga Group

The distribution of stratigraphic ages within the Hyuga Group, cropping out over more than 60 km of width and containing a thin mélange unit on top and alternations of sandstone-rich and mudstone-rich units below, shows throughout its thickness repetitions of a kilometer-scale stratigraphic sequence spanning at most from the late Middle Eocene/early Late Eocene to the Early Oligocene [*Nishi*, 1988; *Sakai et al.*, 1984]. The whole unit is therefore constituted of a single sedimentary sequence accreted many times, probably during a relatively short time lapse, between its youngest stratigraphic ages (Early Oligocene) and crosscutting deformation events, such as movement on the NTL, occurring in the Middle Miocene. Within the Hyuga Mélange, as discussed above, D3, top-to-SE deformation stage is associated with underplating at depth.

5.3.1.2. Nichinan Group

Subsequently to Hyuga Group accretion, the Nichinan Group, lying to the south and structurally below the Hyuga Group, with stratigraphic ages between Late Oligocene and Early Miocene, is also added to the wedge in a second, rapid growth event. The "Early Miocene" stage in Figure 11 depicts the situation after the rapid growth of the prism by addition of Hyuga and Nichinan Group and just before the Takachiho collisional stage described below, where large-scale thrusts, shown as dashed lines, are activated.

5.3.2. Takachiho Phase and Movement on the NTL in Middle Miocene

The Takachiho phase, traditionally described as the major stage of deformation of the Shimanto Belt, is characterized by the unconformity of the Early Miocene (Burdigalian) visible all over Japan [*Charvet and Fabbri*, 1987; *Tanaka and Nozawa*, 1977, and references therein]. In Kyushu, it is apparent as the unconformable deposition of the Miyazaki Group in Late Miocene over the Nichinan Group, the structurally lowest formation of the Shimanto Belt affected by strong folding, with SW-NE trending axes [*Saito et al.*, 1997; *Sakai*, 1985]. Biostratigraphic ages of the Nichinan Group are as young as Early Miocene (see Table 1), so that the Takachiho phase is bracketed in Kyushu between the Early and the late Late Miocene.

Besides, the top-to-SE movement on the NTL [*Kondo et al.*, 2005] can be tightly bracketed: klippes of Cretaceous Shimanto, transported on the NTL, lie above the Hyuga Group (Osuzuyama klippe and Uchinohae klippe) [*Murata,* 1991, 1996, 1998], making the slip on the NTL younger than the Early Oligocene [*Sakai et al.*, 1984]. In addition, the NTL is crosscut by undeformed granites such as the Osuzuyama granite, dated in the Middle Miocene, and the klippes are unconformably overlain by the undeformed Miyazaki Group of the Late Miocene, which places the slip on the NTL between the early Oligocene and the Middle Miocene [*Murata*, 1997]. As a result, we propose to associate the formation of the NTL to the Takachiho phase. Consequently, the combination of the time constraints for the NTL and the Takachiho phase leads to date the movement on the NTL in Middle Miocene.

Geometrically, in our reconstructions (Figure 11, Early Miocene to "present" stage), the movement on the NTL implies displacement on the order of ~50 km, hence results in a large horizontal contraction of the wedge. We have ascribed to the same tectonic stage the formation of the Oyabu Thrust, between the Hyuga Mélange

and the Coherent Hyuga, which is associated with a gap in paleotemperature [*Hara and Kimura*, 2008]. These thrusts are then refolded, probably during ongoing compression, to give the final architecture.

The geodynamical explanation of the Takachiho phase is still debated. Even if large-scale thrusts such as the NTL can be interpretated as out-of-sequence thrusts, similar to those observed in modern margins, this leaves open the question why they formed only during a short time span in the history of the whole belt. *Charvet and Fabbri* [1987] and *Charvet* [2013] proposed that the Takachiho stage (and associated NTL) was caused by the collision with a microcontinental blocks now subducted below the belt, whose presence could explain the isotopic signature of Miocene granitoids [*Jahn*, 2010]. In line with this suggestion, *Stein et al.* [1994] reported the presence, in magmatic bodies, of metamorphic enclaves formed at 0.7–0.8 GPa, best explained by the presence of a continental root below the accretionary prism. Although the absence of outcropping continental crust throughout the Shimanto does not allow to settle the question, we have shown a hypothetical continental sliver in our reconstructions. The continental collision hypothesis, if not yet strongly supported by observations, at least accounts for the peculiarity of this tectonic stage with respect to the long-term evolution of the belt.

5.4. Late-Stage Extension

The D5 faults described here, corresponding to a NW-SE extension, are geometrically and kinematically similar to extensional structures described elsewhere in Kyushu [*Fabbri et al.*, 2004; *Tokushige and Fabbri*, 1996]. On the contrary to what *Fabbri et al.* [2004] propose, in the area we investigated, the extension does not reactivate previous thrusts, but newly formed normal faults cut across earlier thrusts. In the absence of seismic imaging of deep structures, we have conservatively ascribed a limited amplitude to this extension in our reconstructions.

Fabbri et al. [2004] associate this extension to the spreading and rifting of Okinawa Trough [*Letouzey and Kimura*, 1985]. According to *Fabbri et al.* [2004], extension started as early as 13 Ma, i.e., very shortly after Middle Miocene magmatism, to be still active today. Extension is probably spread over the belt, as, on Shikoku, exhumation of deep terranes occurred around 10 Ma, as documented by apatite fission track analyses [*Hasebe and Tagami*, 2001].

6. Conclusion

Our structural study pointed out to the existence, within the northern part of the Shimanto Belt, of several distinct tectonic stages, including a yet unrecognized major phase of extension around 48 Ma. Combined with other structural and paleogeographical data, we associate this event to the subduction of the Pacific-Inazagi Ridge. In the geodynamical scenario developed consequently, the growth of the whole Shimanto Belt does not appear as a steady state process comparable to the models of accretionary prism growth, but rather as the sum of distinct events, with very contrasted kinematic regimes.

Acknowledgments

This work has received funding from the European Research Council (ERC) under the Seventh Framework Programme of the European Union (ERC Advanced Grant, grant agreement 290864, RHEOLITH). We thank Tim Byrne, Satoru Kojima, an anonymous reviewer, and the Associate Editor for their corrections and comments on earlier versions of the manuscript. Field outcrop locations and data used in the maps and stereographic plots are available upon request to the first author.

References

Bangs, N. L., S. P. S. Gulick, and T. H. Shipley (2006), Seamount subduction erosion on the Nankai Trough and its potential impact on the seismogenic zone, *Geology*, *34*(8), 701–704.

Byrne, T., and L. DiTullio (1992), Evidence for changing plate motions in southwest Japan and reconstructions of the Philippine Sea Plate, *Island Arc*, *1*(1), 148–165.

Byrne, T., and D. Fisher (1990), Evidence for a weak and overpressured decollement beneath sediment-dominated accretionary prisms, *J. Geophys. Res.*, *95*(B6), 9081–9097.

Charvet, J. (2013), Late Paleozoic–Mesozoic tectonic evolution of SW Japan: A review – Reappraisal of the accretionary orogeny and revalidation of the collisional model, *J. Asian Earth Sci.*, *72*, 88–101.

Charvet, J., and O. Fabbri (1987), Vue générale sur l'orogenèse Shimanto et l'évolution tertiaire du Japon sud-ouest [in french with english abstract], *Bull. Soc. Geol. Fr.*, *8*, 1171–1188.

Delvaux, D., and B. Sperner (2003), tress tensor inversion from fault kinematic indicators and focal mechanism data: the TENSOR program, in *New Insights Into Structural Interpretation and Modelling*, edited by D. Nieuwland, *Geol. Soc. London Spec. Publ.*, 212, 75–100.

DiTullio, L., and T. Byrne (1990), Deformation paths in the shallow levels of an accretionary prism - The Eocene Shimanto Belt of southwest Japan, *Geol. Soc. Am. Bull.*, *102*(10), 1420–1438.

Dominguez, S., et al. (1998), Upper plate deformation associated with seamount subduction, *Tectonophysics*, *293*, 207–224.

Dominguez, S., J. Malavieille, and S. E. Lallemand (2000), Deformation of accretionary wedges in response to seamount subduction: Insights from sandbox experiments, *Tectonics*, *19*(1), 182–196, doi:10.1029/1999TC900055.

Engebretson, D. C., et al. (1985), *Relative Motions Between Oceanic and Continental Plates in the Pacific Basin*, *Geol. Soc. Am. Spec. Pap.*, *206*, 59 p.

Expedition 316 Scientists (2009), Expedition 316 Site C0007, in *Proc. IODP, 314/315/316*, edited by M. Kinoshita et al., pp. 1-110, Integrated Ocean Drilling Program Management International, Inc., Washington, D. C., doi:110.2204/iodp.proc.314315316.314315135.314312009.
Expedition 319 Scientists (2010), Expedition 319 summary, in *Proc. IODP, 319*, edited by D. Saffer et al., pp. 1–46, Integrated Ocean Drilling Program Management International, Inc., Washington, D. C., doi:10.2204/iodp.proc.2319.2101.2010.
Fabbri, O., J. Charvet, and M. Faure (1987), Phase ductile à vergence nord dans la zone Shimanto de Kyushu (Japon SW), [in french with english abstract], *C. R. Acad. Sci. Paris*, *304*(II), 923–927.
Fabbri, O., et al. (2004), Transtensional deformation at the junction between the Okinawa trough back-arc basin and the SW Japan island arc, in *Vertical Coupling and Decoupling in the Lithosphere*, edited by J. Grocott et al., *Geol. Soc. London Spec. Publ.*, *227*, 297–312.
Faccenna, C., T. W. Becker, S. Lallemand, and B. Steinberger (2012), On the role of slab pull in the Cenozoic motion of the Pacific plate, *Geophys. Res. Lett.*, *39*, L03305, doi:10.1029/2011GL050155.
Faure, M. (1985a), The pre-Cretaceous structure of the outer belt of southwest Japan, *Tectonophysics*, *113*, 139–162.
Faure, M. (1985b), Microtectonic evidence for eastward ductile shear in the Jurassic orogen of SW Japan, *J. Struct. Geol.*, *7*(2), 175–186.
Hara, H., and K. Kimura (2008), Metamorphic cooling history of the Shimanto accretionary complex, Kyushu, southwest Japan: Implications for the timing of out-of-sequence thrusting, *Island Arc*, *17*, 546–559.
Hasebe, N., and T. Tagami (2001), Exhumation of an accretionary prism - results from fission track thermochronology of the Shimanto Belt, southwest Japan, *Tectonophysics*, *331*, 247–267.
Hashimoto, Y., and G. Kimura (1999), Underplating process from melange formation to duplexing: Example from the Cretaceous Shimanto Subbelt, Kii Peninsula, southwest Japan, *Tectonics*, *18*(1), 92–107, doi:10.1029/1998TC900014.
Ikesawa, E., G. Kimura, K. Sato, K. Ikehara-Ohmori, Y. Kitamura, A. Yamaguchi, K. Ujiie, and Y. Hashimoto (2005), Tectonic incorporation of the upper part of oceanic crust to overriding plate of a convergent margin: An example from the Cretaceous-early Tertiary Mugi Melange, the Shimanto Belt, Japan, *Tectonophysics*, *401*(3–4), 217–230.
Imai, I., et al. (1971), Geologic structure and metamorphic zonation of the northeastern part of the Shimanto terrane in Kyushu, Japan [in Japanese with english abstract], *J. Geol. Soc. Jpn.*, *77*, 207–220.
Isozaki, Y., K. Aoki, T. Nakama, and S. Yanai (2010), New insight into a subduction-related orogen: A reappraisal of the geotectonic framework and evolution of the Japanese Islands, *Gondwana Res.*, *18*, 82–105.
Jahn, B. M. (2010), Accretionary orogen and evolution of the Japanese Islands –implications from a Sr–Nd isotopic study of the Phanerozoic granitoids from SW Japan, *Am. J. Sci.*, *310*, 1210–1249.
Kimura, G., and A. Mukai (1991), Underplated unit in an accretionary complex: melange of the Shimanto Belt of eastern Shikoku, southwest Japan, *Tectonics*, *10*, 31–50, doi:10.1029/90TC00799.
Kitamura, Y., et al. (2005), Melange and its seismogenic roof decollement: A plate boundary fault rock in the subduction zone - An example from the Shimanto Belt, Japan, *Tectonics*, *24*, TC5012, doi:10.1029/2004TC001635.
Kondo, H., et al. (2005), Deformation and fluid flow of a major out-of-sequence thrust located at seismogenic depth in an accretionary complex: Nobeoka Thrust in the Shimanto Belt, Kyushu, Japan, *Tectonics*, *24,* TC6008, doi:10.1029/2004TC001655.
Lallemand, S., J. Malavieille, and S. Calassou (1992), Effects of oceanic ridge subduction on accretionary wedges: experimental modeling and marine observations, *Tectonics*, *11*(6), 1301–1313, doi:10.1029/92TC00637.
Letouzey, J., and M. Kimura (1985), Okinawa Trough genesis: Structure and evolution of a backarc basin developed in a continent, *Mar. Petrol. Geol.*, *2*, 111–130.
Lewis, J. C., and T. Byrne (2001), Fault kinematics and past plate motions at a convergent plate boundary: Tertiary Shimanto Belt, southwest Japan, *Tectonics*, *20*(4), 548–565, doi:10.1029/2000TC001239.
Mackenzie, J. S., et al. (1987), Progressive deformation in an accretionary complex: An example from the Shimanto Belt of eastern Kyushu, southwest Japan, *Geology*, *15*, 353–356.
Mackenzie, J. S., et al. (1990), Cleavage dating by K-Ar analysis in the Paleogene Shimanto Belt of eastern Kyushu, S.W. Japan, *J. Min. Petrol. Econ. Geol.*, *85*, 161–167.
Moore, G., et al. (2009), Structural and seismic stratigraphic framework of the NanTroSEIZE Stage 1 transect, in *Proc. IODP, 314/315/316*, edited by M. Kinoshita et al., pp. 1–46, Integrated Ocean Drilling Program Management International, Inc., Washington, D. C., doi:10.2204/iodp.proc.314315316.314315102.314312009.
Moore, G. F., et al. (2001), New insights into deformation and fluid flow processes in the Nankai Trough accretionary prism: Results of Ocean Drilling Program Leg 190, *Geochem. Geophys. Geosyst.*, *2*, 1058, doi:10.1029/2001GC000166.
Moore, G. F., et al. (2005), Legs 190 and 196 synthesis: Deformation and fluid flow processes in the Nankai Trough accretionary prism, in *Proc. ODP, Sci. Results, 190/196*, edited by H. Mikada et al., pp. 1–26, doi:10.2973/odp.proc.sr.190196.190201.192005.
Mukoyoshi, H., et al. (2009), Style of fluid flow and deformation in and around an ancient out-of-sequence thrust: An example from the Nobeoka Tectonic Line ine the Shimanto accretionary complex, southwest Japan, *Island Arc*, *18*, 333–351.
Müller, R. D., et al. (2008), Long-term sea-level fluctuations driven by ocean basin dynamics, *Science*, *319*(1357), 1–7.
Murata, A. (1991), Duplex structures of the Uchinohae Formation in the Shimanto Terrane, Kyushu, Southwest Japan, *J. Geol. Soc. Jpn.*, *97*, 39–52.
Murata, A. (1996), Nappe structures of the Shimanto terrane of the Mikado-Osuzuyama area in East Kyushu [in Japanese with english abstract], *Nat. Sci. Res., Faculty Integrated Arts Sci., The Univ. of Tokushima*, *9*, 49–61.
Murata, A. (1997), Geological map of Miyazaki prefecture, 1:200,000, Miyazaki Prefectural Government.
Murata, A. (1998), Duplexes and low-angle nappe structures of the Shimanto terrane, southwest Japan [in Japanese with english abstract], *Mem. Geol. Soc. Jpn.*, *50*, 147–158.
Nakama, T., et al. (2010), Paleogeography of the japanese islands: Age spectra of detrital zircon and provenance history of the orogen [in japanese with english abstract and figures], *J. Geogr.*, *119*(6), 1161–1172.
Nishi, H. (1988), Structural analysis of the Shimanto accretionary complex, Kyushu, Japan, based on foraminiferal biostratigraphy, *Tectonics*, *7*, 641–652, doi:10.1029/TC007i003p00641.
Ogawauchi, Y., et al. (1984), Stratigraphy and geologic structures of the Shimanto supergroup in the northeastern part of Nobeoka city, Miyazaki Prefecture, Japan, *Bull. Fac. Sci. Kagoshima Univ.*, *17*, 67–88.
Onishi, C. T., G. Kimura, Y. Hashimoto, K. Ikehara-Ohmori, and T. Watanabe (2001), Deformation history of tectonic melange and its relationship to the underplating process and relative plate motion: An example from the deeply buried Shimanto Belt, SW Japan, *Tectonics*, *20*(3), 376–393, doi:10.1029/1999TC001154.
Platt, J. P. (1986), Dynamics of orogenic wedges and the uplift of high-pressure metamorphic rocks, *Geol. Soc. Am. Bull.*, *97*, 1037–1053.
Raimbourg, H., S. Tadahiro, Y. Asuka, Y. Haruka, and G. Kimura (2009), Horizontal shortening versus vertical loading in accretionary prisms, *Geochem. Geophys. Geosyst.*, *10,* Q04007, doi:10.1029/2008GC002279.

Sage, F., J.-Y. Collot, and C. R. Ranero (2006), Interplate patchiness and subduction-erosion mechanisms: Evidence from depth-migrated seismic images at the central Ecuador convergent margin, *Geology*, *34*(12), 997–1000.
Saito, M., et al. (1996), *Geological Map of Japan, 1:50,000*, Geol. Surv. Jpn., Shiibamura.
Saito, M., et al. (1997), *Geological Map of Japan, 1:200,000*, Geol. Surv. Jpn., Miyazaki.
Sakaguchi, A. (1999), Thermal structure and paleo-heat flow in the Shimanto accretionary prism, Southwest Japan, *Island Arc*, *8*, 359–372.
Sakai, A., and K. Kanmera (1981), Stratigraphy of the Shimanto terrane and the tectono-stratigraphic setting of the greenstones of the northern part of Miyazaki prefecture, Kyushu, *Sci. Rep. Dep. Geol. Kyushu Univ.*, *14*, 31–48.
Sakai, T. (1985), Geology of the Nichinan Group and the process of production of the outermargin olisthostrome belt of the Shimanto terrane [in Japanese with english abstract], in *Mem. Symp. on Formation of Slump Facies and their Relationship to Tectonics, some Problems on the Deformation of Unconsolidated Sediments*, edited, pp. 95–116, Tsukuba, Tsukuba Univ., Japan.
Sakai, T., et al. (1984), Microfossil stratigraphy of the Paleogene system in Kyushu Shimanto Belt [in Japanese with english abstract], in *Biostratigraphy and International Correlation of the Paleogene System in Japan*, edited by T. Saito et al., pp. 95–112, Yamagata Univ., Yamagata, Japan.
Sakamoto, T. (1977), Neogene systems, in *Geology and Mineral Resources of Japan*, edited by K. Tanaka and T. Nozawa, pp. 233–259, Geol. Surv. Jpn., Tsukuba, Japan.
Shibata, K. (1978), Contemporaneity of Tertiary granites in the Outer Zone of Southwest Japan, *Bull. Geol. Surv. Jpn.*, *29*, 551–554.
Shibata, K., and T. Nozawa (1982), Radiometric age map, granitic rocks, scale 1/4 000 000, in *Geological Atlas of Japan*, edited by Geol. Surv. Jpn., pp. 66–67, Tsukuba, Japan.
Stein, G., et al. (1994), Geodynamic setting of volcano-plutonic rocks in so-called "paleo-accretionary prisms": Fore-arc activity or post-collisional magmatism? The Shimanto Belt as a case study, *Lithos*, *33*, 85–107.
Tagami, T., and C. Shimada (1996), Natural long-term annealing of the zircon fission track system around a granitic pluton, *J. Geophys. Res.*, *101*(B4), 8245–8255, doi:10.1029/95JB02885.
Taira, A. (1981), The Shimanto Belt of southwest Japan and arc-trench sedimentary tectonics, *Recent Prog. Nat. Sci. Jpn.*, *6*, 147–162.
Taira, A., et al. (1980a), The geology of the Shimanto Belt in Kochi prefecture, Shikoku, in *Geology and paleontology of the Shimanto Belt*, edited by A. Taira and H. Tashiro, pp. 319–389, Rinyo Kosaikai Press, Kochi.
Taira, A., et al. (1980b), Lithofacies and geologic age relationship within mélange zones of northern Shimanto Belt (Cretaceous), Kochi prefecture, in *Geology and paleontology of the Shimanto Belt*, edited by A. Taira and H. Tashiro, pp. 319–389, Rinyo Kosaikai Press, Kochi.
Taira, A., et al. (1988), The Shimanto Belt in Shikoku, Japan--Evolution of Cretaceous to Miocene accretionary prism, *Mod. Geol.*, *12*, 5–46.
Tanaka, K., and T. Nozawa (1977), *Geology and Mineral Resources of Japan*, 430 pp., Geol. Surv. Jpn., Tsukuba, Japan.
Teraoka, Y., and K. Okumura (1992), Tectonic division and Cretaceous sandstone compositions of the Northern Belt of the Shimanto Terrane, southwest Japan, *Mem. Geol. Soc. Jpn.*, *38*, 261–270.
Teraoka, Y., et al. (1981), *Geological Map of Japan, 1:200,000*, Geol. Surv. Jpn., Nobeoka.
Teraoka, Y., et al. (1990), *Geological Map of Japan, 1:50,000*, Geol. Surv. Jpn., Saiki.
Teraoka, Y., K. Shibata, K. Okumura, and S. Uchiumi (1994), K-Ar ages of detrital K-feldspars and muscovites from the Shimanto Supergroup in east Kyushu and west Shikoku, southwest Japan [in Japanese with english abstract], *J. Geol. Soc. Jpn.*, *100*(7), 477-485.
Tokushige, H., and O. Fabbri (1996), Mesofaults and associated stress field in the Late Miocene to Pliocene forearc deposits of the Miyazaki district, southeast Kyushu, Japan, *J. Geol. Soc. Jpn.*, *102*(7), 622–634.
Toriumi, M., and J. Teruya (1988), Tectono-metamorphism of the Shimanto Belt, *Mod. Geol.*, *12*, 303–324.
Von Blanckenburg, F., and J. H. Davies (1995), Slab breakoff: A model for syncollisional magmatism and tectonics in the Alps, *Tectonics*, *14*(1), 120–131, doi:10.1029/94TC02051.
Von Huene, R., and S. Lallemand (1990), Tectonic erosion along the Japan and Peru convergent margins, *GSA Bull.*, *102*(6), 704–720.
Von Huene, R., and D. W. Scholl (1991), Observations at convergent margins concerning sediment subduction, subduction erosion, and the growth of continental crust, *Rev. Geophys.*, *29*(3), 279–316, doi:10.1029/91RG00969.
Wallis, S. (1998), Exhuming the Sambagawa metamorphic belt: The importance of tectonic discontinuities, *J. Metamorph. Geol.*, *16*, 83–95.
Whittaker, J. M., et al. (2007), Major Australian-Antartic plate reorganization at Hawaiian-Emperor Bend time, *Science*, *318*(83), 1–5.